Drug Design, Development and Therapy

Dovepress
open access to scientific and medical research

Open Access Full Text Article

ORIGINAL RESEARCH

Proteomic response to 5,6-dimethylxanthenone 4-acetic acid (DMXAA, vadimezan) in human non-small cell lung cancer A549 cells determined by the stable-isotope labeling by amino acids in cell culture (SILAC) approach

This article was published in the following Dove Press journal:
Drug Design, Development and Therapy
17 February 2015
Number of times this article has been viewed

Shu-Ting Pan,[1,*] Zhi-Wei Zhou,[2,3,*] Zhi-Xu He,[3] Xueji Zhang,[4] Tianxin Yang,[5] Yin-Xue Yang,[6] Dong Wang,[7] Jia-Xuan Qiu,[1] Shu-Feng Zhou[2]

[1]Department of Oral and Maxillofacial Surgery, The First Affiliated Hospital of Nanchang University, Nanchang, Jiangxi, People's Republic of China; [2]Department of Pharmaceutical Sciences, College of Pharmacy, University of South Florida, Tampa, FL, USA; [3]Guizhou Provincial Key Laboratory for Regenerative Medicine, Stem Cell and Tissue Engineering Research Center and Sino-US Joint Laboratory for Medical Sciences, Guiyang Medical University, Guiyang, [4]Research Center for Bioengineering and Sensing Technology, University of Science and Technology Beijing, Beijing, People's Republic of China; [5]Department of Internal Medicine, University of Utah and Salt Lake Veterans Affairs Medical Center, Salt Lake City, UT, USA; [6]Department of Colorectal Surgery, General Hospital of Ningxia Medical University, Yinchuan, [7]Cancer Center, Daping Hospital and Research Institute of Surgery, Third Military Medical University, Chongqing, People's Republic of China

*These two authors contributed equally to this work

Correspondence: Shu-Feng Zhou
Department of Pharmaceutical Sciences, College of Pharmacy, University of South Florida, 12901 Bruce B. Downs Boulevard, Tampa, FL 33612, USA
Tel +1 813 974 6276
Fax +1 813 905 9885
Email szhou@health.usf.edu

Jia-Xuan Qiu
Department of Oral and Maxillofacial Surgery, The First Affiliated Hospital of Nanchang University, 17 Yongwaizheng St, Nanchang 330006, Jiangxi, People's Republic of China
Tel +86 791 8869 5069
Fax +86 791 8869 2745
Email qiujiaxuan@163.com

Abstract: 5,6-Dimethylxanthenone 4-acetic acid (DMXAA), also known as ASA404 and vadimezan, is a potent tumor blood vessel-disrupting agent and cytokine inducer used alone or in combination with other cytotoxic agents for the treatment of non-small cell lung cancer (NSCLC) and other cancers. However, the latest Phase III clinical trial has shown frustrating outcomes in the treatment of NSCLC, since the therapeutic targets and underlying mechanism for the anticancer effect of DMXAA are not yet fully understood. This study aimed to examine the proteomic response to DMXAA and unveil the global molecular targets and possible mechanisms for the anticancer effect of DMXAA in NSCLC A549 cells using a stable-isotope labeling by amino acids in cell culture (SILAC) approach. The proteomic data showed that treatment with DMXAA modulated the expression of 588 protein molecules in A549 cells, with 281 protein molecules being up regulated and 306 protein molecules being downregulated. Ingenuity pathway analysis (IPA) identified 256 signaling pathways and 184 cellular functional proteins that were regulated by DMXAA in A549 cells. These targeted molecules and signaling pathways were mostly involved in cell proliferation and survival, redox homeostasis, sugar, amino acid and nucleic acid metabolism, cell migration, and invasion and programed cell death. Subsequently, the effects of DMXAA on cell cycle distribution, apoptosis, autophagy, and reactive oxygen species (ROS) generation were experimentally verified. Flow cytometric analysis showed that DMXAA significantly induced G_1 phase arrest in A549 cells. Western blotting assays demonstrated that DMXAA induced apoptosis via a mitochondria-dependent pathway and promoted autophagy, as indicated by the increased level of cytosolic cytochrome c, activation of caspase 3, and enhanced expression of beclin 1 and microtubule-associated protein 1A/1B-light chain 3 (LC3-II) in A549 cells. Moreover, DMXAA significantly promoted intracellular ROS generation in A549 cells. Collectively, this SILAC study quantitatively evaluates the proteomic response to treatment with DMXAA that helps to globally identify the potential molecular targets and elucidate the underlying mechanism of DMXAA in the treatment of NSCLC.

Keywords: DMXAA, non-small cell lung cancer, cell cycle, apoptosis, autophagy, SILAC

Introduction

Lung cancer is the most common cancer and the leading cause of cancer-related death in humans worldwide.[1,2] There were about 1.8 million new cases diagnosed with lung cancer in 2012, accounting for 12.9% of the total cases of cancer.[1,2] Small-cell lung cancer and non-small cell lung cancer (NSCLC) are the two major types of lung cancer. NSCLC is the most common type, accounting for 70%–85% of all cases of lung cancer. In the USA, there were 207,339 new cases of lung cancer and 156,953 deaths resulting

from lung cancer in 2011,[3] and it is estimated that there were 224,210 new cases of lung cancer and 159,260 deaths due to lung cancer in 2014.[4] In the People's Republic of China, lung cancer is the most common cancer and the leading cause of cancer-related death, with a skyrocketing increase in incidence and mortality rates.[2,5] In 2009, the incidence rate for lung cancer was about 53.57/100,000, accounting for 18.74% of overall new cases of cancer; the mortality rate for lung cancer was about 45.57/100,000, accounting for 25.24% of cancer-related deaths.[2,5] Current therapies for lung cancer include surgery, chemotherapy, radiotherapy, immunotherapy, and targeted therapy, which are used alone or in combination. However, the therapeutic outcome for lung cancer is often disappointing, in particular for advanced NSCLC,[6,7] due to the poor response to current therapeutics, drug resistance, and severe side effects, which highlights an urgent need for discovery of efficacious and safe new agents for the treatment of NSCLC.

5,6-Dimethylxanthenone-4-acetic acid (DMXAA, Figure 1), also known as vadimezan and ASA404, is a vascular-disrupting agent that reduces the blood supply to tumoral tissue, resulting in tumor regression.[8,9] However, the molecular targets and exact mechanisms of action of DMXAA are elusive so far. DMXAA shows inhibitory effects against several protein kinases, with the most potent effects being on the vascular endothelial growth factor receptor tyrosine kinase family.[10,11] DMXAA is a potent inducer of tumor necrosis factor-α and activates host immune effectors that assist in killing cancer cells.[10] DMXAA induces rapid vascular collapse and subsequent tumor hemorrhagic necrosis via induction of apoptosis in tumor vascular endothelial cells

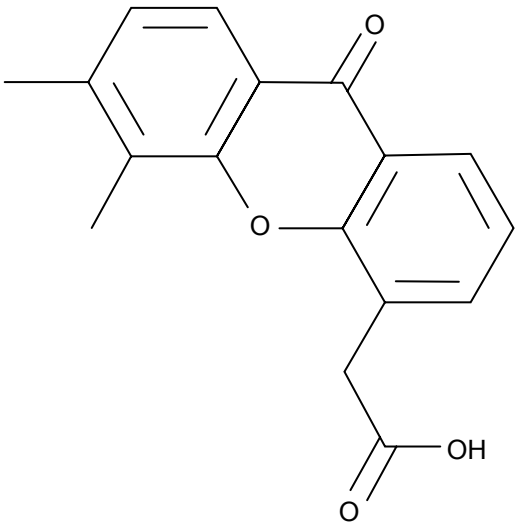

Figure 1 Chemical structure of 5,6-dimethylxanthenone 4-acetic acid (DMXAA).

and indirect vascular effects induced by various cytokines, in particular, tumor necrosis factor-α, serotonin, and nitric oxide.[10] The pharmacokinetics of DMXAA has also be investigated. In cancer patients, DMXAA concentration-time profiles are well described by a three-compartment model with saturable elimination.[12] Body surface area and sex are significant covariates on the volume of distribution of the central compartment and the maximum elimination rate, respectively.[12] DMXAA is extensively metabolized in human liver microsomes and cancer patients. There are two major metabolites of DMXAA, ie, DMXAA acyl glucuronide and 6-hydroxymethyl-5-methylxanthenone-4-acetic acid (6-OH-MXAA). Cytochrome P450 1A2 is responsible for the conversion of DMXAA to 6-OH-MXAA, with an apparent K_m of 6.2 μM and a V_{max} of 0.014 nmol/minute/mg.[13] DMXAA is also extensively metabolized by uridine 5'-diphosphoglucuronosyltransferase 1A2 (UGT1A2) and UGT2B7, with a greater contribution from UGT2B7.[14] DMXAA has been tested mainly in the treatment of NSCLC, and also in prostate cancer and human epidermal growth factor receptor 2-negative breast cancer.[15–20] In these clinical studies, DMXAA is used alone and more often in combination with other cytotoxic drugs. A Phase II clinical trial showed that DMXAA in combination with carboplatin and paclitaxel had a potent anticancer effect in NSCLC patients.[15] This triple combination therapy prolonged the survival of about 5 months when compared with the monotherapy.[15] However, the Phase III clinical trial conducted by Lara et al showed that the triple chemotherapy of DMXAA with carboplatin and paclitaxel failed to improve the efficacy of the monotherapy.[16] This may be due to the complexity of the mechanisms of action of DMXAA. DMXAA has been shown to target the stimulator of interferon gene (STING) pathway and this effect is only observed in mice but not in humans.[21–23] However, this cannot provide a convincing explanation for the failure of DMXAA in the Phase III trial in NSCLC patients. Therefore, it is of great importance to globally understand and uncover the molecular targets and related signaling pathways involved in the anticancer effect of DMXAA and DMXAA-based combination therapies.

So far, there are many studies on the mechanisms of action of DMXAA in the treatment of NSCLC, showing that DMXAA can activate STING-dependent innate immune pathways and mitogen-activated protein kinases and inhibit vascular endothelial growth factor receptor.[11,21–23] However, there is a lack of evidence to depict the global molecular targets and related signaling pathways for the NSCLC cell killing effects of DMXAA, such as cell proliferation, programmed

cell death, and cell migration and invasion. Notably, targeting cell cycle progression, apoptosis, autophagy, and epithelial to mesenchymal transition (EMT) has been proposed for treatment of NSCLC.[24] Therefore, an approach that can evaluate cellular proteomic responses to the DMXAA is important for the optimal treatment of NSCLC. Stable-isotope labeling by amino acids in cell culture (SILAC) is a practical and powerful approach to uncovering the global proteomic response to drug treatment and other interventions.[25] In particular, it can be used to systemically and quantitatively assess the target network of drugs, to evaluate drug toxicity, and to identify new biomarkers for the diagnosis and treatment of important diseases, including NSCLC.[25–27] In this regard, we investigated the molecular targets of DMXAA in A549 cells using a combination of proteomic and functional approaches, with a focus on cell cycle distribution, apoptosis, autophagy, and redox homeostasis.

Materials and methods

Chemicals and reagents

DMXAA (purity ≥98%), $^{13}C_6$-L-lysine, L-lysine, $^{13}C_6$ $^{15}N_4$-L-arginine, L-arginine, RNase A, propidium iodide, Dulbecco's phosphate-buffered saline (PBS), heat-inactivated fetal bovine serum (FBS), dialyzed FBS, and Roswell Park Memorial Institute (RPMI)-1640 medium for SILAC were purchased from Sigma-Aldrich Co. (St Louis, MO, USA). The 5-(and 6)-chloromethyl-2′,7′-dichlorodihydrofluorescein diacetate (CM-H_2DCFDA) was sourced from Invitrogen Inc. (Carlsbad, CA, USA). A FASP™ protein digestion kit was purchased from Protein Discovery Inc. (Knoxville, TN, USA). RPMI-1640 medium for general cultural use was obtained from Corning Cellgro Inc. (Herndon, VA, USA). The polyvinylidene difluoride membrane was purchased from EMD Millipore Inc. (Bedford, MA, USA). Proteomic quantitation kits for acidification, desalting, and digestion, ionic detergent compatibility reagent, a Pierce bicinchoninic acid protein assay kit, and Western blotting substrate were obtained from Thermo Fisher Scientific Inc. (Waltham, MA, USA). Primary antibodies against human cytochrome c, cleaved caspase 3, microtubule-associated protein 1A/1B-light chain 3-I (LC3-I), LC3-II, and beclin 1 were all purchased from Cell Signaling Technology Inc. (Beverly, MA, USA). The antibody against human β-actin was obtained from Santa Cruz Biotechnology Inc. (Dallas, TX, USA).

Cell line and cell culture

The A549 NSCLC cell line was obtained from American Type Culture Collection (Manassas, VA, USA) and cultured in RPMI-1640 medium supplemented with 10% heat-inactivated FBS. The cells were maintained at 37°C in a 5% CO_2/95% air humidified incubator. DMXAA was dissolved in dimethyl sulfoxide at a stock concentration of 20 mM and stored at −20°C. It was freshly diluted to predetermined concentrations with culture medium. The final concentration of dimethyl sulfoxide was 0.05% (v/v). The control cells received the vehicle only.

Quantitative proteomic study using SILAC

Quantitative proteomic experiments were performed using a SILAC-based approach as described previously.[25,26,28] Briefly, A549 cells were cultured in RPMI-1640 medium (for SILAC) with (heavy) or without (light) stable isotope-labeled amino acids ($^{13}C_6$ L-lysine and $^{13}C_6$ $^{15}N_4$ L-arginine) and 10% dialyzed FBS. A549 cells cultured in heavy medium were treated with 10 μM DMXAA for 24 hours after six cell doubling times. After treatment with DMXAA, A549 cell samples were harvested and lysed with hot lysis buffer (100 mM Tris base, 4% sodium dodecyl sulfate [SDS], and 100 mM dithiothreitol). The cell lysate was denatured at 95°C for 5 minutes and then sonicated for 3 seconds with six pulses. The samples were then centrifuged at 15,000× *g* for 20 minutes at room temperature and the supernatant was collected. The protein concentration was determined using ionic detergent compatibility reagent. Subsequently, equal amounts of heavy and light protein samples were combined to reach a total volume of 30–60 μL containing 300–600 μg protein. The combined protein sample was digested using an filter-aided sample prep (FASP™) protein digestion kit. After digestion, the resulting sample was acidified to a pH of 3 and desalted using a C_{18} solid-phase extraction column. The samples were then concentrated using a vacuum concentrator at 45°C for 120 minutes, and the peptide mixtures (5 μL) were subjected to the hybrid linear ion trap (LTQ Orbitrap XL™, Thermo Fisher Scientific Inc.). Liquid chromatography-tandem mass spectrometry was performed using a 10 cm long, 75 μm (inner diameter) reversed-phase column packed with 5 μm diameter C_{18} material having a pore size of 300 Å (New Objective Inc., Woburn, MA, USA) with a gradient mobile phase of 2%–40% acetonitrile in 0.1% formic acid at 200 μL per minute for 125 minutes. The Orbitrap full mass spectrometry scanning was performed at a mass (*m/z*) resolving power of 60,000, with positive polarity in profile mode ($M + H^+$). The peptide SILAC ratio was calculated using MaxQuant version 1.2.0.13. The SILAC ratio was determined by averaging all peptide SILAC ratios from peptides identified of the same

protein. The proteins were identified using Scaffold 4.3.2 (Proteome Software Inc., Portland, OR, USA) and the pathway was analyzed using ingenuity pathway analysis (IPA) from QIAGEN Inc. (Redwood City, CA, USA).

Cell cycle analysis using flow cytometry

The effect of treatment with DMXAA on the cell cycle was determined by flow cytometry as described previously.[29] Briefly, A549 cells were treated with DMXAA at concentrations of 0.1, 1, and 10 μM for 24 hours. In separate experiments, A549 cells were treated with 10 μM DMXAA over a 72-hour period. The cells were suspended, fixed in 70% ethanol, washed in PBS, and resuspended in 1 mL of PBS containing 1 mg/mL RNase A and 50 μg/mL propidium iodide. The cells were incubated in the dark for 30 minutes at room temperature. Next, the cells were subject to cell cycle analysis using a flow cytometer (BD LSR II Analyzer; Becton Dickinson Immunocytometry Systems, San Jose, CA, USA). The flow cytometer collected 10,000 events for analysis.

Measurement of intracellular reactive oxygen species (ROS) levels

Intracellular levels of ROS were measured by a fluorometer using CM-H_2DCFDA according to the manufacturer's instructions. Cell-permeant CM-H_2DCFDA passively diffuses into cells and is retained in the cells after cleavage by intracellular esterases. Upon oxidation by ROS, the nonfluorescent CM-H_2DCFDA is converted to highly fluorescent CM-DCF. Briefly, A549 cells were seeded into a 96-well plate at a density of 1×10^4 cells/well. After treatment with DMXAA at 0.1, 1, and 10 μM for 48 hours, the cells were incubated with CM-H_2DCFDA at 5 μM in PBS for 30 minutes. The fluorescence intensity was detected at wavelengths of 485 nm (excitation) and 530 nm (emission). The control cells were treated with vehicle only (0.05% dimethyl sulfoxide, v/v).

Western blotting analysis

A549 cells were washed with pre-cold PBS after 24-hour treatment with DMXAA at 0.1, 1, and 10 μM, lysed with radioimmunoprecipitation (RIPA) buffer containing the protease inhibitor and phosphatase inhibitor cocktails, and centrifuged at 3,000× *g* for 10 minutes at 4°C. Protein concentrations were measured using a Pierce bicinchoninic acid protein assay kit. An equal amount of protein sample (30 μg) was resolved by SDS polyacrylamide gel electrophoresis (PAGE) sample loading buffer and electrophoresed on 12% SDS-PAGE minigel after thermal denaturation at 95°C for 5 minutes. The proteins were transferred onto an Immobilon polyvinylidene difluoride membrane at 400 mA for 1 hour at 4°C. Membranes were blocked with skim milk and probed with the indicated primary antibody overnight at 4°C and then blotted with appropriate horseradish peroxidase-conjugated secondary anti-mouse or anti-rabbit antibody. Visualization was performed using a ChemiDoc™ XRS system (Bio-Rad, Hercules, CA, USA) with enhanced chemiluminescence substrate, and the blots were analyzed using Image Lab 3.0 (Bio-Rad). The protein level was normalized to the matching densitometric value of the internal control β-actin.

Statistical analysis

The data are presented as the mean ± standard deviation (SD). Comparisons of multiple groups were evaluated by one-way analysis of variance (ANOVA) followed by Tukey's multiple comparison procedure. Values of $P<0.05$ were considered to be statistically significant. Assays were performed at least three times independently.

Results

Overview of proteomic response to DMXAA treatment in A549 cells

To reveal the potential molecular targets of DMXAA in the treatment of NSCLC, we conducted proteomic experiments to evaluate the interactome of DMXAA in A549 cells. There were 588 protein molecules identified as potential molecular targets of DMXAA in A549 cells, with 281 protein molecules being upregulated and 306 protein molecules being downregulated (Table 1). Subsequently, these proteins were subjected to IPA. The results showed that 256 signaling pathways and 184 cellular functional proteins were regulated by DMXAA in A549 cells (Tables 2 and 3). These functional proteins were involved in a number of important cellular processes, including cell proliferation, redox homeostasis, cell metabolism, cell migration and invasion, cell survival, and cell death. The signaling pathways included the G_1 and G_2 checkpoint regulation pathways, the phosphatidylinositol-4,5-bisphosphate 3-kinase (PI3K)/Akt/mammalian target of rapamycin (mTOR)signaling pathway, the 5′-AMP-activated protein kinase (AMPK) signaling pathway, the nuclear factor erythroid 2-related factor 2 (Nrf2)-mediated oxidative stress response pathway, the epithelial adherens junction signaling pathway, regulation of the epithelial-mesenchymal transition signaling pathway, the nuclear factor-κB signaling pathway, and the apoptosis signaling pathway. The IPA results showed that the top ten targeted signaling pathways were the eukaryotic initiation factor

Table 1 The 588 protein molecules regulated by DMXAA (5,6-dimethylxanthenone 4-acetic acid) in A549 cells

Protein ID/symbol	Molecular weight (kDa)	Normalized heavy/light ratio
Q5VXJ5	93.115	0.036825
P3C2G	165.71	0.052938
K1C10	58.826	0.090984
K1C9	62.064	0.11756
CB067	73.235	0.14108
1433F	28.218	0.22201
K1C14	51.561	0.33079
K2C1	66.038	0.3831
F5H2G2	52.909	0.43495
K2C6B	60.066	0.4391
MANF	20.7	0.52102
F8VVM2	36.161	0.56761
APMAP	32.161	0.59766
KRT85	55.802	0.59966
B4DS13	64.805	0.60022
F5H6E3	18.467	0.62881
E9PEU4	47.204	0.65669
E9PF80	25.3	0.65828
F5H3I4	34.557	0.66102
AL3A2	54.847	0.71801
RAB1B	22.171	0.71899
F5GY65	28.494	0.71909
ISG15	17.887	0.71998
ACACA	257.24	0.72374
H90B4	58.264	0.72926
K22E	65.432	0.73358
F5H0X6	50.435	0.73677
F8VSA6	5.8668	0.73947
AK1C1	36.788	0.74328
RLA1	11.514	0.74644
B4DKS8	37.255	0.75044
TMOD3	39.594	0.75127
BASP1	22.693	0.75558
COX2	25.565	0.77367
MARCS	31.554	0.77387
F8WD96	30	0.77581
F5GX11	26.505	0.77779
K2C8	53.704	0.78215
K1C18	48.057	0.7824
FKB1A	11.951	0.78264
B4E1K7	33.337	0.7835
Q5TCU6	258.08	0.784
RL29	17.752	0.78622
F8W7P7	72.716	0.78997
CHM4B	24.95	0.79348
E9PNH1	13.163	0.79972
C9JW37	8.8333	0.79997
CLCC1	39.837	0.80061
B4E241	14.203	0.80205
E9PH29	25.838	0.80339
NNMT	29.574	0.80458
E7ESM6	101.21	0.80816
RL36	12.254	0.80826
ETFB	27.843	0.81589
F5GWR2	26.63	0.81598
SC61B	9.9743	0.81767
ALDR	35.853	0.81844
AK1C2	36.735	0.81875
GRHPR	35.668	0.81892
PON2	37.996	0.82002
B7Z254	47.837	0.82473
FRIL	20.019	0.82759
ATP5H	18.491	0.82832
B4DNJ5	43.368	0.82967
HINT1	13.802	0.83028
D6RDN3	4.1286	0.83128
S10A4	11.728	0.83154
CUL4B	102.3	0.83195
IDHC	46.659	0.83275
E9PDQ8	41.438	0.83332
F8W914	37.144	0.83563
ANXA4	35.882	0.83679
S38A2	45.178	0.837
F5H3T8	52.305	0.84001
CDC37	44.468	0.84082
A6NKT1	56.36	0.84176
B4E0X8	66.231	0.84218
SMRD2	55.238	0.84281
F8WF81	14.275	0.84585
RRBP1	108.63	0.84762
SFPQ	76.149	0.85165
B4DRT4	17.326	0.85394
B4DT43	30.025	0.85426
KHDR1	44.027	0.8553
E9PPQ5	20.723	0.85913
D6RFI0	21.504	0.8613
CDC42	21.258	0.86162
COX41	19.576	0.86224
EF1A2	50.47	0.86292
SCMC1	51.354	0.86294
C9J1T2	9.4459	0.86457
GBG12	8.0061	0.8649
E9PKD1	47.431	0.86946
C9JPV1	12.063	0.86969
BLVRB	22.119	0.86996
F5H4L5	32.734	0.87025
K2C7	51.385	0.87164
FKBP3	25.177	0.87335
F5H1J1	38.739	0.87421
ECH1	35.816	0.87427
EFTU	49.541	0.87443
AL1A1	54.861	0.8745
RAB5C	23.482	0.8745
D6RFH4	14.846	0.87485
HSPB1	22.782	0.8751
G6PD	59.256	0.87609
RB11A	24.393	0.87617
HCD2	26.923	0.8781
CALX	67.567	0.87892
B1AHC7	64.075	0.87955
F5H7G7	57.342	0.88015
CAZA1	32.922	0.88192
S100P	10.4	0.88323

(*Continued*)

Table 1 (*Continued*)

Protein ID/symbol	Molecular weight (kDa)	Normalized heavy/light ratio
AK1C3	36.853	0.88425
CALR	48.141	0.88565
NOP2	88.972	0.88741
HMGA1	11.676	0.88955
F8W6V8	53.116	0.88964
MIF	12.476	0.89038
USMG5	6.4575	0.89172
PSB2	22.836	0.89303
CBR1	30.375	0.8935
SF3B3	44.605	0.89353
PRDX5	17.031	0.89389
LRRF1	82.688	0.89483
B4DQJ8	51.872	0.89714
CCNK	41.293	0.9026
FSCN1	54.529	0.90332
CS021	75.356	0.90345
B4E022	62.878	0.90614
G3V5P4	16.916	0.90639
PDIA4	72.932	0.90743
KYNU	52.351	0.90767
PRS6B	43.507	0.90881
D6RF62	37.111	0.90967
S10A6	10.18	0.91026
F5GYB8	19.471	0.91104
B3KUK2	19.73	0.91118
PPIB	23.742	0.91132
D6REM6	88.358	0.91208
F2Z3A5	40.127	0.91256
R13AX	12.134	0.91339
SRSF1	22.46	0.91352
GRP78	72.332	0.91353
F2Z2J9	28.85	0.91353
DNJA2	45.745	0.91354
RS19	16.06	0.91521
RL23A	17.695	0.91665
B7Z2V6	37.751	0.91676
TMED9	27.277	0.91682
IMUP	8.5115	0.91694
ENPL	92.468	0.917
LKHA4	57.299	0.91952
SERC	35.188	0.91971
B1AM77	13.475	0.92027
F5GYG9	76.233	0.92196
D6RF44	12.64	0.92222
B4E0R6	109.36	0.9266
MDHM	35.503	0.92738
RS15	17.04	0.92751
AL3A1	50.394	0.92795
ATPB	56.559	0.92872
Q5T8U3	21.545	0.93039
LGUL	19.043	0.93096
A8K318	59.177	0.93162
CH10	10.932	0.93233
CYTB	11.139	0.9324
C8KIM0	47.267	0.93263
G3V5Q1	27.125	0.93343
RS14	16.273	0.93344

(*Continued*)

Table 1 (*Continued*)

Protein ID/symbol	Molecular weight (kDa)	Normalized heavy/light ratio
A6NN01	12.146	0.93348
B7Z6M1	65.632	0.93372
B3KUB4	31.857	0.93524
NUDC	38.242	0.9354
FAS	273.42	0.93581
F5GWY2	58.615	0.93612
SMD2	13.527	0.93633
MDHC	36.426	0.93699
B4DIT7	68.648	0.93774
D6RFJ8	47.291	0.9383
E9PRQ6	15.159	0.93879
FIS1	16.937	0.93901
SAHH	47.716	0.93913
RLA2	11.665	0.93935
AATM	47.517	0.93946
INF2	134.62	0.93976
ATPA	59.75	0.93996
HNRPG	42.331	0.94001
EIF1	12.732	0.94212
C9JPM4	14.553	0.94439
ARF1	20.697	0.94471
FLNB	275.66	0.945
NSF1C	28.522	0.94549
CDV3	22.079	0.94575
E7EWF1	45.498	0.94724
NDKB	30.137	0.94913
B1AH77	16.775	0.95
H2A1J	13.936	0.95043
GDIR1	23.207	0.95062
LDHB	36.638	0.95153
PA1B3	25.734	0.95246
HNRPU	88.979	0.95295
G3V3I1	16.645	0.95297
F2Z3F8	29.245	0.95333
B4DVU3	88.161	0.95514
HSP74	94.33	0.9556
B4DKM5	27.478	0.95717
SPRE	28.048	0.9575
B4DEM7	57.645	0.95821
F5GX39	13.631	0.95862
F5GZ27	85.64	0.96103
PRDX1	22.11	0.96121
PTBP1	57.221	0.96124
F5H667	83.267	0.9617
C9JLU1	16.996	0.96193
B4DR70	44.812	0.96206
SMD1	13.281	0.9621
E7EU12	94.863	0.96289
E7ETK5	30.611	0.96294
B4DXW1	42.003	0.9639
RCN1	38.89	0.96394
PABP1	61.18	0.96407
ANXA1	38.714	0.96409
PARK7	19.891	0.96461
H12	21.364	0.96469
B7Z6A4	14.854	0.96516
F8VNT9	14.265	0.96517

(*Continued*)

Table 1 (*Continued*)

Protein ID/symbol	Molecular weight (kDa)	Normalized heavy/light ratio
E9PKZ0	22.389	0.96545
F5H1S2	18.845	0.96676
LRC59	34.93	0.96685
UGDH	55.023	0.96807
TPIS	26.669	0.96808
ROA2	37.429	0.96842
VDAC1	30.772	0.96869
KPYM	57.936	0.96936
ANXA5	35.936	0.96942
UBE2N	17.138	0.96961
ENOA	47.168	0.97022
S10AA	11.203	0.97031
HN1	16.014	0.97056
PPIA	18.012	0.9708
RL12	17.818	0.97093
F5GZ16	99.271	0.97167
TCPA	60.343	0.97176
B4DRF4	36.43	0.97231
ILF2	43.062	0.9728
PDCD5	14.285	0.97482
XPO2	22.67	0.97527
RLA0	34.273	0.9763
B4DZP4	45.004	0.97635
F8W810	50.529	0.97677
B3KQT9	54.102	0.97689
E5RJR5	18.72	0.97695
CAP1	51.901	0.97716
A8K3Z3	44.784	0.97817
B4DUR8	55.674	0.9785
C9JV57	13.025	0.97853
E7EMJ6	31.455	0.97864
RS17L	15.55	0.97906
F5H8J3	75.177	0.97909
RS9	22.591	0.97946
LDHA	36.688	0.97949
HNRDL	27.191	0.97974
B7Z4V2	72.4	0.98075
CKAP4	66.022	0.9808
PDIA1	57.116	0.98205
AT2A2	109.73	0.98343
LPPRC	157.9	0.98408
TALDO	37.54	0.98454
PHB2	33.296	0.98512
NBAS	254.81	0.9852
F5GY50	32.895	0.98539
RS4X	29.597	0.98585
B4DPJ8	54.867	0.98615
SYEP	170.59	0.98633
HNRPC	27.821	0.98649
EF1A1	50.14	0.98718
D6RG13	25.608	0.98723
AK1BA	36.019	0.98779
EF1G	50.118	0.98818
NAMPT	55.52	0.98886
F8VTY8	41.746	0.98925
C9JTK6	12.302	0.9895
TCPE	59.67	0.98993
RS18	17.718	0.99091
FKBP4	51.804	0.99111

(*Continued*)

Table 1 (*Continued*)

Protein ID/symbol	Molecular weight (kDa)	Normalized heavy/light ratio
MOES	67.819	0.99187
ARP2	44.76	0.99233
RS5	22.876	0.99268
RL11	20.124	0.99323
F8VRG3	6.4352	0.99333
C9JZ20	22.27	0.99398
C9JB50	7.888	0.99449
DX39A	49.129	0.9946
F5GYN4	28.05	0.99464
B7Z795	47.709	0.99535
B7Z4T9	54.804	0.99554
TERA	89.321	0.99599
TCP4	14.395	0.99621
B4DGN5	46.575	0.99641
DBPA	31.947	0.99662
ADT2	32.852	0.99664
CALM	16.837	0.99736
PGK1	44.614	0.99895
ECHM	31.387	0.99951
MARE1	29.999	0.99998
RS7	22.127	1
API5	49.496	1.0009
1433G	28.302	1.0011
IQGA1	189.25	1.0015
B4DDF7	64.181	1.0018
LETM1	83.353	1.0024
E7EWI9	34.102	1.0027
D6RAS3	23.383	1.0035
B4DLR8	22.793	1.0053
PROF1	15.054	1.0054
ALO17	118.43	1.0056
RS3	26.688	1.0064
RAB10	22.541	1.0066
XRCC5	82.704	1.0076
UBA1	117.85	1.0076
CH60	61.054	1.0081
A6NLM8	16.245	1.0083
F8W0A9	40.793	1.0086
NONO	54.231	1.0087
C9J7S3	19.969	1.0092
C1QBP	31.362	1.0099
D6RAN4	20.874	1.0103
PDC6I	96.022	1.0107
B4E3C2	17.094	1.0115
MAP4	85.251	1.0117
GSTP1	23.356	1.0129
RL10A	24.831	1.0129
ACTS	42.051	1.0141
DHX9	140.96	1.0146
PCBP1	37.497	1.0146
F5H1W0	55.907	1.0147
H33	15.328	1.0156
RS6	28.68	1.0164
G3V279	8.2033	1.0169
D6RBT8	23.862	1.0179
PRDX6	25.035	1.0193
CAND1	136.37	1.0201

(*Continued*)

Table 1 (*Continued*)

Protein ID/symbol	Molecular weight (kDa)	Normalized heavy/light ratio
TCTP	19.595	1.0203
B4DDG1	14.121	1.0204
C9JCK5	18.607	1.0216
PSB3	22.949	1.022
MAP1B	270.63	1.0222
CN166	28.068	1.0223
ACTN4	104.85	1.0228
E9PQD7	25.211	1.0232
E7EX53	15.722	1.0241
B7ZAT2	52.717	1.026
PAIRB	42.426	1.0261
E9PCY7	47.087	1.0262
HNRPK	48.562	1.0268
B8ZZQ6	11.758	1.0272
ACOC	98.398	1.0274
IF5A1	16.832	1.0284
B4E335	39.226	1.0286
PCNA	28.768	1.0288
A6NL93	9.5355	1.0294
FLNA	280.01	1.0304
Q5JR95	21.879	1.0308
C9J9K3	29.505	1.0309
E7ETA0	34.028	1.0312
TBB4B	49.83	1.0315
COF1	18.502	1.0318
CLIC1	26.922	1.0322
RINI	49.973	1.0325
1433E	29.174	1.033
C9JF49	6.6566	1.0331
RS13	17.222	1.0332
GUAA	76.715	1.0333
AN32B	22.276	1.0342
E9PGI8	20.18	1.0342
CLCA	23.662	1.0345
DYHC1	532.4	1.035
E9PMD7	28.898	1.035
1433T	27.764	1.0354
E9PEN3	29.353	1.0367
CLH1	187.89	1.0371
E9PFH8	41.824	1.0377
G3V3T3	21.126	1.0378
GDIB	50.663	1.0384
PALLD	73.321	1.04
B1ALW1	9.4519	1.0404
A8MUD9	24.433	1.0407
NDKA	17.149	1.0422
Q2YDB7	16.541	1.0422
S10AB	11.74	1.0434
QCR2	48.442	1.0437
RS10	18.898	1.0446
B7Z9L0	52.33	1.0449
G3P	36.053	1.046
E7EQR4	65.578	1.046
GBLP	35.076	1.0464
1433B	27.85	1.0465
F5H0N0	37.406	1.0468
G6PI	63.146	1.0478
E7EUG1	71.178	1.0499
EF1B	24.763	1.0504
H4	11.367	1.0504

(*Continued*)

Table 1 (*Continued*)

Protein ID/symbol	Molecular weight (kDa)	Normalized heavy/light ratio
BTF3	17.699	1.0505
PGRC2	23.818	1.0508
F8W118	24.694	1.051
H32	15.388	1.0514
DYL2	10.35	1.0516
E9PEC0	32.819	1.0516
ALDOA	39.42	1.0522
EF2	95.337	1.0523
TBA1C	49.895	1.0528
IPYR	32.66	1.054
F8VZJ2	15.016	1.0547
PRS10	44.172	1.0559
F8W7K3	282.14	1.0567
H2B1L	13.952	1.0571
G3V5B3	19.154	1.058
HSP71	70.051	1.0588
B2REB8	30.992	1.0591
B4DR63	41.167	1.0595
RL22	14.787	1.0599
ACTN1	103.06	1.06
B4E2S7	39.811	1.0605
G3V5M3	9.2044	1.0608
C9JU56	13.336	1.061
B7Z1N6	35.423	1.0625
CAN2	79.994	1.0631
F8VWC5	18.091	1.0641
SODC	15.936	1.0644
TBA1B	50.151	1.0646
RS16	16.445	1.065
C9JD32	9.6694	1.0658
VINC	116.72	1.0668
RS25	13.742	1.0671
A4D177	20.811	1.0685
Q5HYE7	20.42	1.0694
GLRX3	37.432	1.0699
B4E3E8	71.354	1.0717
LEG1	14.716	1.0729
A8K8G0	22.964	1.0736
TPM4	28.521	1.0744
F5H897	74.267	1.0744
E9PJH8	15.461	1.0749
E9PNR9	18.297	1.0749
F8W181	25.892	1.0756
AIBP	20.43	1.0758
HSP7C	70.897	1.076
CPNS1	28.315	1.0764
ANXA2	38.604	1.0765
1433Z	27.745	1.077
HS90A	84.659	1.0771
C9JKI3	15.928	1.0779
HNRPL	64.132	1.0786
NPM	29.464	1.0788
AHNK	629.09	1.079
F8VYX6	48.46	1.0796
EF1D	31.121	1.0797
GTF2I	107.97	1.0801
D6R9P3	30.302	1.0806
PSME1	28.723	1.0815
Q8N1C0	59.549	1.0838
ADT3	32.866	1.0863
B4DY66	19.152	1.087

(*Continued*)

Table 1 (*Continued*)

Protein ID/symbol	Molecular weight (kDa)	Normalized heavy/light ratio
PLEC	531.78	1.0874
E7EX81	65.881	1.0877
C9J712	9.7982	1.088
F6RFD5	15.397	1.0883
PSME2	27.401	1.09
HS90B	83.263	1.0909
F5H4D6	31.451	1.0914
B4DR31	58.162	1.0921
RS12	14.515	1.0928
TADBP	27.972	1.0948
B6EAT9	37.277	1.0972
RS15A	14.839	1.0986
RS20	13.373	1.1055
B4E3S0	41.603	1.108
RS28	7.8409	1.1109
LMNA	74.139	1.1139
ROA1	29.386	1.1144
PGRC1	21.671	1.1155
C9JHS6	5.6564	1.1161
Q5TA01	20.938	1.1186
TIF1B	79.473	1.1193
HNRPM	73.62	1.1205
RL19	23.466	1.1208
TXNL1	32.251	1.1218
RAN	24.423	1.1235
F8W7C6	18.592	1.1241
G3XAI4	119.77	1.1248
IF4A1	46.153	1.1252
VIME	53.651	1.1263
F5H0T1	59.777	1.1272
C9JFR7	11.333	1.1279
E7EPB3	14.558	1.1287
DDX5	69.147	1.1298
F5H6Q2	13.789	1.1306
ITB1	87.445	1.1347
B4DP24	29.485	1.135
TAGL2	22.391	1.1361
B3KS31	41.952	1.1361
SPTB2	251.39	1.1366
G3V531	44.06	1.1371
PYGB	96.695	1.141
PRP8	273.6	1.1413
DNJA1	44.868	1.1421
TBB2B	49.953	1.1428
HNRPQ	58.735	1.1433
B7Z9C4	35.253	1.1444
IMB1	97.169	1.1455
F8W0G4	16.637	1.1455
KINH	109.68	1.1465
F8WBE5	8.8809	1.1471
METK2	43.66	1.1482
PTRF	33.362	1.1512
K6PP	85.595	1.1514
B7Z2S5	60.021	1.1531
B2RDM2	36.177	1.1541
B4DSC0	14.503	1.1554
ECHA	82.999	1.1555
F8VPF3	14.436	1.1565
B0V3J0	26.101	1.159
F8VR50	9.7261	1.1619
B3KTM6	28.044	1.1649
BAF	10.058	1.1652
IF2A	36.112	1.1676
Q5H907	55.795	1.1682
TPM1	32.876	1.1693
IF6	26.599	1.1727
SYTC	83.434	1.1736
Q75MH1	12.985	1.1814
B4DZI8	99.045	1.1821
Q5T4L4	7.3564	1.1834
Q5T093	13.439	1.1877
H31	15.404	1.1882
Q5VU59	27.174	1.1982
TBB4A	49.585	1.1987
MYH9	226.53	1.2006
IMA2	57.861	1.2074
GLSK	65.459	1.2081
Q5T7C4	18.311	1.2156
C9JFK9	34.759	1.2186
G3V153	70.353	1.223
PSA7	20.193	1.2257
E5RHS5	26.635	1.2275
1433S	27.774	1.2337
F2Z3D0	8.1111	1.238
PSA4	29.483	1.2384
B7Z8D3	14.761	1.2419
B4E2Z3	55.939	1.2474
E9PP21	16.94	1.25
ROA0	30.84	1.2609
B4DMT5	33.24	1.2628
C9K0U8	14.131	1.2706
UBP15	112.42	1.2708
ML12A	19.794	1.2917
LASP1	29.717	1.2975
A8MUB1	48.328	1.2985
APOL2	37.092	1.304
HMOX1	32.818	1.3048
PSA3	27.647	1.312
TYB10	5.0256	1.3172
Q5T4B6	5.1127	1.3249
C9IZ41	17.054	1.3258
F5H4W0	44.933	1.331
LAT1	55.01	1.3337
PSB1	26.489	1.335
B4DPJ6	17.473	1.34
F5H0C8	34.762	1.3474
TBB3	50.432	1.3583
TBAL3	45.517	1.4041
DUT	17.748	1.4353
F8WC15	47.819	1.4365
PLIN3	28.157	1.4972
F5GWR9	22.218	1.499
C9JL85	5.7044	1.5138
E7ERP8	31.801	1.5322
AAAT	56.598	1.6533
RBM3	17.17	1.7162
B4DP11	16.476	1.8007
MYOF	179.55	1.9046
SRP14	14.57	1.9407
PLP2	16.691	NaN
HNF4A	52.784	NaN
YLPM1	241.64	NaN
E7EWZ6	111.13	NaN
Q5TCU3	32.814	NaN

Table 2 Signaling pathways for target proteins regulated by DMXAA (5,6-dimethylxanthenone 4-acetic acid) in A549 cells

Ingenuity canonical pathways	–Log*P*	Molecules
eIF2 signaling	2.11E01	EIF3C, AKT2, RPS3A, RPS27, RPS2, RPL17, RPS8, RPL23, EIF3E, RPL9, RPL7, RPL15, RPL14, RPL8, EIF3F, RPL7A, RPL28, RPS26, RPL5, RPL10, PPP1CA, RPL31, RPL18, RPL13, RPSA
mTOR signaling	7.52E00	AKT2, EIF3C, RPS3A, RPS27, RPS2, RPS8, EIF3E, EIF3F, PPP2R1A, RPS26, RHOA, RPSA, EIF4B
Regulation of eIF4 and p70S6K signaling	6.82E00	AKT2, EIF3F, PPP2R1A, EIF3C, RPS3A, RPS26, RPS27, RPS2, RPS8, EIF3E, RPSA
Epithelial adherens junction signaling	5.87E00	AKT2, ACTR3, TUBB6, MYL6, ACTB, RHOA, TUBA4A, CTNNA1, ARPC3, ZYX
Remodeling of epithelial adherens junctions	5.43E00	ACTR3, TUBB6, ACTB, TUBA4A, CTNNA1, ARPC3, ZYX
Nrf2-mediated oxidative stress response	5.05E00	GSR, SOD2, STIP1, ACTB, NQO1, CCT7, TXN, PTPLAD1, TXNRD1, GSTO1
RhoA signaling	4.66E00	ACTR3, CFL2, MYL6, EZR, ACTB, RHOA, PFN2, ARPC3
Integrin signaling	4.62E00	RAC2, AKT2, ACTR3, ARF4, ACTB, RHOA, CAV1, ARPC3, ZYX, TLN1
Regulation of actin-based motility by Rho	4.59E00	RAC2, ACTR3, MYL6, ACTB, RHOA, PFN2, ARPC3
Fcγ receptor-mediated phagocytosis in macrophages and monocytes	4.53E00	RAC2, AKT2, ACTR3, EZR, ACTB, ARPC3, TLN1
Actin cytoskeleton signaling	4.35E00	RAC2, ACTR3, CFL2, MYL6, EZR, ACTB, RHOA, PFN2, ARPC3, TLN1
Axonal guidance signaling	4.17E00	DPYSL2, RAC2, AKT2, MYL6, PDIA3, TUBA4A, ACTR3, TUBB6, CFL2, RHOA, RTN4, ARPC3, PFN2, PSMD14
Purine nucleotides de novo biosynthesis II	3.88E00	IMPDH2, PAICS, ATIC
Germ cell-Sertoli cell junction signaling	3.83E00	RAC2, TUBB6, CFL2, ACTB, RHOA, TUBA4A, CTNNA1, ZYX
Protein ubiquitination pathway	3.77E00	PSMA6, PSMC1, UBE2L3, HSPA9, PSMD14, PSMA1, UBC, PSMA2, SKP1, PSMC5
RhoGDI signaling	3.6E00	ACTR3, CFL2, MYL6, EZR, ACTB, RHOA, CD44, ARPC3
Inosine-5′-phosphate biosynthesis II	3.57E00	PAICS, ATIC
Vitamin C transport	3.55E00	TXN, TXNRD1, GSTO1
Huntington's disease signaling	3.44E00	TGM2, CTSD, AKT2, CYCS, CPLX2, HSPA9, POLR2H, UBC, PSME3
RAN signaling	3.28E00	TNPO1, XPO1, IPO5
Thioredoxin pathway	2.88E00	TXN, TXNRD1
Superoxide radical degradation	2.88E00	SOD2, NQO1
Gluconeogenesis I	2.78E00	ENO2, ME1, ALDOC
Integrin linked kinase signaling	2.69E00	AKT2, PPP2R1A, CFL2, MYL6, ACTB, RHOA, NACA
Aryl hydrocarbon receptor signaling	2.65E00	TGM2, CTSD, NEDD8, NQO1, PTGES3, GSTO1
Leukocyte extravasation signaling	2.54E00	RAC2, MYL6, EZR, ACTB, RHOA, CD44, CTNNA1
Rac signaling	2.5E00	ACTR3, CFL2, RHOA, CD44, ARPC3
Gap junction signaling	2.43E00	AKT2, TUBB6, PDIA3, ACTB, CAV1, TUBA4A
Pentose phosphate pathway	2.33E00	PGD, TKT
Caveolar-mediated endocytosis signaling	2.31E00	ARCN1, ACTB, CAV1, COPB2
Tight junction signaling	2.28E00	AKT2, PPP2R1A, MYL6, ACTB, RHOA, CTNNA1
Ephrin receptor signaling	2.19E00	RAC2, AKT2, ACTR3, CFL2, RHOA, ARPC3
Ceramide signaling	2.15E00	CTSD, AKT2, PPP2R1A, CYCS
Signaling by Rho family GTPases	2.15E00	ACTR3, CFL2, MYL6, EZR, ACTB, RHOA, ARPC3
Sertoli cell-Sertoli cell junction signaling	2.13E00	AKT2, TUBB6, ACTB, CAV1, TUBA4A, CTNNA1
Virus entry via endocytic pathways	1.99E00	RAC2, ACTB, CAV1, TFRC
Antioxidant action of vitamin C	1.86E00	PDIA3, TXN, TXNRD1, GSTO1
Semaphorin signaling in neurons	1.86E00	DPYSL2, CFL2, RHOA
Actin nucleation by ARP-WASP complex	1.79E00	ACTR3, RHOA, ARPC3
Glutamate biosynthesis II	1.72E00	GLUD1

Glutamate degradation X	1.72E00	GLUD1
Glycolysis I	1.63E00	ENO2, ALDOC
Mitochondrial dysfunction	1.62E00	GSR, PRDX3, SOD2, CYCS, VDAC2
14-3-3-mediated signaling	1.59E00	AKT2, TUBB6, PDIA3, TUBA4A
Pyrimidine ribonucleotide interconversion	1.57E00	CMPK1, CTPS1
Ascorbate recycling (cytosolic)	1.55E00	GSTO1
Glutathione redox reactions II	1.55E00	GSR
Thyroid hormone biosynthesis	1.55E00	CTSD
4-aminobutyrate degradation I	1.55E00	SUCLG2
Pigment epithelium derived factor signaling	1.52E00	AKT2, SOD2, RHOA
Pyrimidine ribonucleotide biosynthesis de novo	1.51E00	CMPK1, CTPS1
Clathrin-mediated endocytosis signaling	1.5E00	ACTR3, ACTB, TFRC, ARPC3, UBC
Ephrin B signaling	1.49E00	RAC2, CFL2, RHOA
Breast cancer regulation by stathmin1	1.45E00	PPP2R1A, TUBB6, RHOA, TUBA4A, PPP1CA
Arsenate detoxification I (glutaredoxin)	1.43E00	GSTO1
Uracil degradation II (reductive)	1.43E00	DPYSL2
2-ketoglutarate dehydrogenase complex	1.43E00	DLST
Thymine degradation	1.43E00	DPYSL2
Cell cycle regulation by BTG family proteins	1.36E00	PPP2R1A, PRMT1
tRNA splicing	1.36E00	TSEN34, APEX1
Pentose phosphate pathway (oxidative branch)	1.33E00	PGD
Glutamate degradation III (via 4-aminobutyrate)	1.33E00	SUCLG2
Focal adhesion kinase signaling	1.3E00	AKT2, ACTB, TLN1
Docosahexaenoic acid signaling	1.28E00	AKT2, CYCS
tRNA charging	1.28E00	RARS, DARS
Arginine biosynthesis IV	1.25E00	GLUD1
Pentose phosphate pathway (nonoxidative branch)	1.25E00	TKT
Citrulline-nitric oxide cycle	1.25E00	CAV1
Death receptor signaling	1.24E00	ACIN1, CYCS, ACTB
Mechanisms of viral exit from host cells	1.24E00	ACTB, XPO1
Telomerase signaling	1.17E00	AKT2, PPP2R1A, PTGES3
Hypoxia-inducible factor-1α signaling	1.13E00	AKT2, CAV1, APEX1
Cdc42 signaling	1.12E00	ACTR3, CFL2, MYL6, ARPC3
Ephrin A signaling	1.12E00	CFL2, RHOA
Wnt/β-catenin signaling	1.11E00	AKT2, PPP2R1A, CD44, UBC
Prostanoid biosynthesis	1.08E00	PTGES3
Sucrose degradation V (mammalian)	1.08E00	ALDOC
Ketolysis	1.08E00	ACAT1
Sphingosine-1-phosphate signaling	1.07E00	AKT2, PDIA3, RHOA
Retinoic acid receptor activation	1.06E00	AKT2, RPL7A, PSMC5, PRMT1
Endometrial cancer signaling	1.06E00	AKT2, CTNNA1
Ketogenesis	1.04E00	ACAT1

(Continued)

Table 2 (*Continued*)

Ingenuity canonical pathways	–LogP	Molecules
Production of nitric oxide and reactive oxygen species in macrophages	1.03E00	AKT2, PPP2R1A, RHOA, PPP1CA
Lymphotoxin β receptor signaling	1.03E00	AKT2, CYCS
Hereditary breast cancer signaling	1.02E00	AKT2, POLR2H, UBC
Glutaryl-CoA degradation	1E00	ACAT1
Gα12/13 signaling	9.98E-01	AKT2, MYL6, RHOA
Glioma invasiveness signaling	9.91E-01	RHOA, CD44
Regulation of cellular mechanics by calpain protease	9.91E-01	EZR, TLN1
CD28 signaling in T-helper cells	9.9E-01	AKT2, ACTR3, ARPC3
ERK/MAPK signaling	9.87E-01	RAC2, PPP2R1A, TLN1, PPP1CA
Glucocorticoid receptor signaling	9.85E-01	HMGB1, AKT2, HSPA9, POLR2H, PTGES3
p70S6K signaling	9.82E-01	AKT2, PPP2R1A, PDIA3
Myc-mediated apoptosis signaling	9.79E-01	AKT2, CYCS
High-mobility group box 1 signaling	9.74E-01	HMGB1, AKT2, RHOA
Thrombin signaling	9.63E-01	AKT2, MYL6, PDIA3, RHOA
Induction of apoptosis by human immunodeficiency virus-1	9.54E-01	CYCS, SLC25A3
Xenobiotic metabolism signaling	9.34E-01	PPP2R1A, CES1, NQO1, PTGES3, GSTO1
Cell cycle: G_1/S checkpoint regulation	9.08E-01	RPL5, SKP1
Cellular effects of sildenafil (Viagra®)	9.05E-01	MYL6, PDIA3, ACTB
Isoleucine degradation I	9.03E-01	ACAT1
Urate biosynthesis/inosine 5′-phosphate degradation	9.03E-01	IMPDH2
Mevalonate pathway I	9.03E-01	ACAT1
Hypoxia signaling in the cardiovascular system	8.97E-01	UBE2L3, NQO1
Cardiac β-adrenergic signaling	8.76E-01	PPP2R1A, PPP1CA, APEX1
Chondroitin sulfate degradation (metazoa)	8.75E-01	CD44
Superpathway of citrulline metabolism	8.75E-01	CAV1
Agrin interactions at neuromuscular junction	8.55E-01	RAC2, ACTB
Granzyme B signaling	8.49E-01	CYCS
Dermatan sulfate degradation (metazoa)	8.49E-01	CD44
Methionine degradation I (to homocysteine)	8.49E-01	PRMT1
Parkinson's signaling	8.49E-01	CYCS
Renal cell carcinoma signaling	8.35E-01	AKT2, UBC
Small-cell lung cancer signaling	8.35E-01	AKT2, CYCS
Endothelial nitric oxide synthase signaling	8.22E-01	AKT2, HSPA9, CAV1
Synaptic long-term depression	8.16E-01	PPP2R1A, PDIA3, CAV1
Leptin signaling in obesity	8.07E-01	AKT2, PDIA3
Glutathione redox reactions I	8.02E-01	GSR
Superpathway of geranylgeranyldiphosphate biosynthesis I (via mevalonate)	8.02E-01	ACAT1
Cysteine biosynthesis III (mammalia)	8.02E-01	PRMT1
Glioblastoma multiforme signaling	7.91E-01	AKT2, PDIA3, RHOA

DNA damage-induced 14-3-3σ signaling	7.8E-01	AKT2
Cyclins and cell cycle regulation	7.71E-01	PPP2R1A, SKP1
Dopamine receptor signaling	7.71E-01	PPP2R1A, PPP1CA
Granzyme A signaling	7.6E-01	APEX1
Purine nucleotide degradation II (aerobic)	7.6E-01	IMPDH2
Tryptophan degradation III (eukaryotic)	7.6E-01	ACAT1
C-X-C-motif chemokine receptor-4 signaling	7.55E-01	AKT2, MYL6, RHOA
Polyamine regulation in colon cancer	7.23E-01	PSME3
Pyrimidine deoxyribonucleotide biosynthesis I de novo	7.23E-01	CMPK1
Phospholipase C signaling	7.15E-01	TGM2, PEBP1, MYL6, RHOA
Thyroid hormone receptor/retinoid X receptor activation	7.14E-01	AKT2, ME1
Tricarboxylic acid cycle II (eukaryotic)	7.05E-01	DLST
Dopamine-DARPP32 feedback in cAMP signaling	7.05E-01	PPP2R1A, PDIA3, PPP1CA
Cytotoxic T-lymphocyte antigen 4 signaling in cytotoxic T lymphocytes	6.91E-01	AKT2, PPP2R1A
Gβγ signaling	6.91E-01	AKT2, CAV1
Ultraviolet-induced MAPK signaling	6.91E-01	CYCS, PDIA3
Interleukin-22 signaling	6.89E-01	AKT2
Tumoricidal function of hepatic natural killer cells	6.89E-01	CYCS
Crosstalk between dendritic cells and natural killer cells	6.84E-01	ACTB, TLN1
p21-activated kinase signaling	6.84E-01	CFL2, MYL6
Apoptosis signaling	6.84E-01	ACIN1, CYCS
Triacylglycerol degradation	6.73E-01	CES1
Vascular endothelial growth factor signaling	6.7E-01	AKT2, ACTB
Lipid antigen presentation by CD1	6.58E-01	PDIA3
Antiproliferative role of TOB in T-cell signaling	6.58E-01	SKP1
cAMP response element-binding protein signaling in neurons	6.54E-01	AKT2, PDIA3, POLR2H
Salvage pathways of pyrimidine ribonucleotides	6.49E-01	AKT2, CMPK1
Interleukin-15 production	6.44E-01	TWF1
B-cell receptor signaling	6.3E-01	RAC2, AKT2, CFL2
Glutathione-mediated detoxification	6.3E-01	GSTO1
Amyotrophic lateral sclerosis signaling	6.22E-01	CYCS, SSR4
Calcium signaling	6.21E-01	MYL6, TPM3, ASPH
Superpathway of cholesterol biosynthesis	6.16E-01	ACAT1
CDK5 signaling	6.16E-01	PPP2R1A, PPP1CA
Nitric oxide signaling in the cardiovascular system	6.16E-01	AKT2, CAV1
Interleukin-8 signaling	5.98E-01	RAC2, AKT2, RHOA
Paxillin signaling	5.98E-01	ACTB, TLN1
Superpathway of methionine degradation	5.91E-01	PRMT1
Cytotoxic T lymphocyte-mediated apoptosis of target cells	5.8E-01	CYCS
Molecular mechanisms of cancer	5.74E-01	RAC2, AKT2, CYCS, RHOA, CTNNA1
Agranulocyte adhesion and diapedesis	5.73E-01	MYL6, EZR, ACTB
Nerve growth factor signaling	5.68E-01	AKT2, RHOA

(*Continued*)

Table 2 (*Continued*)

Ingenuity canonical pathways	–LogP	Molecules
N-formyl-l-methionyl-l-leucyl-phenylalanine signaling in neutrophils	5.63E-01	ACTR3, ARPC3
Fc epsilon RI signaling	5.57E-01	RAC2, AKT2
TNF-related weak inducer of apoptosis signaling	5.57E-01	CYCS
Inhibition of angiogenesis by thrombospondin 1	5.57E-01	AKT2
Retinol biosynthesis	5.57E-01	CES1
Natural killer cell signaling	5.52E-01	RAC2, AKT2
Role of tissue factor in cancer	5.52E-01	AKT2, CFL2
Triacylglycerol biosynthesis	5.47E-01	ELOVL1
Stearate biosynthesis I (animals)	5.47E-01	ELOVL1
Nucleotide excision repair pathway	5.47E-01	POLR2H
Antigen presentation pathway	5.26E-01	PDIA3
Protein kinase A signaling	5.21E-01	MYL6, PDIA3, RHOA, PPP1CA, APEX1
CCR3 signaling in eosinophils	5.15E-01	CFL2, RHOA
Phosphatase and tensin homolog signaling	5.1E-01	RAC2, AKT2
Netrin signaling	5.07E-01	RAC2
Synaptic long-term potentiation	5.05E-01	PDIA3, PPP1CA
P2Y purigenic receptor signaling pathway	5.05E-01	AKT2, PDIA3
Sperm motility	5.01E-01	TWF1, PDIA3
Role of protein kinase R in interferon induction and antiviral response	4.98E-01	CYCS
PI3K/Akt signaling	4.86E-01	AKT2, PPP2R1A
Melanoma signaling	4.81E-01	AKT2
Estrogen receptor signaling	4.68E-01	POLR2H, HNRNPD
PI3K signaling in B lymphocytes	4.64E-01	AKT2, PDIA3
Ovarian cancer signaling	4.51E-01	AKT2, CD44
Cardiac hypertrophy signaling	4.49E-01	MYL6, PDIA3, RHOA
Role of Oct4 in mammalian embryonic stem cell pluripotency	4.49E-01	PHB
Macrophage stimulating protein-RON signaling pathway	4.49E-01	ACTB
Insulin receptor signaling	4.39E-01	AKT2, PPP1CA
Relaxin signaling	4.35E-01	AKT2, APEX1
5′-AMP-activated protein kinase signaling	4.35E-01	AKT2, PPP2R1A
TNF receptor-1 signaling	4.27E-01	CYCS
Cell cycle: G^2/M DNA damage checkpoint regulation	4.27E-01	SKP1
Assembly of RNA polymerase II complex	4.2E-01	POLR2H
Amyloid processing	4.14E-01	AKT2
CD27 signaling in lymphocytes	4.07E-01	CYCS
Interleukin-2 signaling	4.01E-01	AKT2
Gαq signaling	3.89E-01	AKT2, RHOA
Role of checkpoint kinase 1 proteins in cell cycle checkpoint control	3.89E-01	PPP2R1A
Epidermal growth factor signaling	3.83E-01	AKT2
Nur77 signaling in T lymphocytes	3.77E-01	CYCS

Phospholipases	3.77E-01	PDIA3
Aldosterone signaling in epithelial cells	3.72E-01	PDIA3, HSPA9
Tec kinase signaling	3.53E-01	ACTB, RHOA
Estrogen-dependent breast cancer signaling	3.5E-01	AKT2
Granulocyte-monocyte colony stimulating factor signaling	3.5E-01	AKT2
Retinoic acid mediated apoptosis signaling	3.4E-01	CYCS
Interleukin-17A signaling in airway cells	3.4E-01	AKT2
Pyridoxal 5′-phosphate salvage pathway	3.4E-01	AKT2
Non-small cell lung cancer signaling	3.35E-01	AKT2
Interleukin-15 signaling	3.3E-01	AKT2
Angiopoietin signaling	3.3E-01	AKT2
Mitotic roles of polo-like kinase	3.3E-01	PPP2R1A
Role of PI3K/Akt signaling in the pathogenesis of influenza	3.3E-01	AKT2
Pregnane X receptor/9-cis retinoic acid receptor activation	3.25E-01	AKT2
Erythropoietin signaling	3.25E-01	AKT2
Gamma aminobutyric acid receptor signaling	3.25E-01	UBC
Role of MAPK signaling in the pathogenesis of influenza	3.21E-01	AKT2
Macropinocytosis signaling	3.21E-01	RHOA
Acute phase response signaling	3.2E-01	AKT2, SOD2
Role of NFAT in regulation of immune response	3.15E-01	AKT2, XPO1
Endothelin-1 signaling	3.12E-01	PDIA3, CAV1
Melatonin signaling	3.12E-01	PDIA3
Interleukin-3 signaling	3.07E-01	AKT2
Chemokine signaling	3.07E-01	RHOA
Interleukin-17 signaling	3.03E-01	AKT2
Janus kinase/Stat signaling	3.03E-01	AKT2
Nuclear factor kappaB activation by viruses	2.99E-01	AKT2
FLT3 signaling in hematopoietic progenitor cells	2.95E-01	AKT2
Toll-like receptor signaling	2.95E-01	UBC
Dendritic cell maturation	2.94E-01	AKT2, PDIA3
Role of NFAT in cardiac hypertrophy	2.94E-01	AKT2, PDIA3
Triggering receptor expressed on myeloid cells 1 signaling	2.91E-01	AKT2
HER-2 signaling in breast cancer	2.87E-01	AKT2
VEGF family ligand-receptor interactions	2.87E-01	AKT2
Interleukin-4 signaling	2.87E-01	AKT2
Acute myeloid leukemia signaling	2.83E-01	AKT2
Platelet-derived growth factor signaling	2.83E-01	CAV1
Regulation of the epithelial to mesenchymal transition pathway	2.81E-01	AKT2, RHOA
$1,25(OH)_2D$/retinoid X receptor	2.79E-01	PSMC5
Role of macrophages, fibroblasts, and endothelial cells in rheumatoid arthritis	2.68E-01	AKT2, PDIA3, RHOA
Prostate cancer signaling	2.65E-01	AKT2

(*Continued*)

Table 2 (*Continued*)

Ingenuity canonical pathways	–Log*P*	Molecules
Fibroblast growth factor signaling	2.55E-01	AKT2
Neuregulin signaling	2.45E-01	AKT2
RANK signaling in osteoclasts	2.45E-01	AKT2
Chronic myeloid leukemia signaling	2.3E-01	AKT2
Stress-activated protein/Janus kinase signaling	2.27E-01	RAC2
Glioma signaling	2.24E-01	AKT2
Mouse embryonic stem cell pluripotency	2.24E-01	AKT2
Insulin-like growth factor 1 signaling	2.19E-01	AKT2
p53 signaling	2.16E-01	AKT2
Neuropathic pain signaling in dorsal horn neurons	2.11E-01	PDIA3
Cholecystokinin/gastrin-mediated signaling	2.08E-01	RHOA
Hepatocyte growth factor signaling	1.98E-01	AKT2

Abbreviations: ARP, actin-related protein; cAMP, cyclic adenosine monophosphate; ERK, extracellular signal-regulated kinase; MAPK, mitogen-activated protein kinase; PI3K, phosphatidylinositol-4,5-bisphosphate 3-kinase; NFAT, nuclear factor of activated T-cells; TNF, tumor necrosis factor; VEGF, vascular endothelial growth factor; WASP, Wiskott-Aldrich syndrome protein.

(eIF) 2 signaling pathway, mTOR signaling pathway, eIF4 and p70S6K signaling pathway, epithelial adherens junction signaling pathway, remodeling of epithelial adherens junctions pathway, Nrf2-mediated oxidative stress response signaling pathway, RhoA signaling pathway, integrin signaling pathway, Rho-mediated regulation of actin-based motility signaling pathway, and Fcγ receptor-mediated phagocytosis signaling pathway (Table 2).

DMXAA modulates networked signaling pathways in A549 cells

As seen in Figures 2 and 3, DMXAA showed an ability to regulate a number of networked signaling pathways that have critical roles in the regulation of cellular processes. IPA classified the top ten networks of signaling pathways responding to DMXAA in A549 cells (Table 4). These signaling networks have important roles in pathophysiological functions and the development of many important diseases. They included gene expression, DNA replication, recombination and repair, protein synthesis, small molecule biochemistry, carbohydrate metabolism, lipid metabolism, energy production, cellular response to therapeutics, connective tissue development and function, cellular assembly and organization, cellular compromise, cell morphology, free radical scavenging, cell death and survival, neurological disease, skeletal and muscular disorders, cardiac damage, cardiac fibrosis, development and function of cardiovascular system, and development of cancer.

DMXAA modulates important regulators involved in cell cycle distribution in A549 cells

It has been reported that regulation of cell cycle distribution is an effective approach in the treatment of lung cancer,[24] and that vascular-disrupting agents exhibit modulating effects on cell cycle distribution. However, it has not been fully uncovered the molecular targets and underlying mechanisms of DMXAA. Therefore, in order to explore the effect and potential molecular targets of DMXAA on cell cycle distribution in A549 cells, we treated A549 cells with 10 μM DMXAA for 24 hours and then subjected samples of the cells to quantitative proteomic analysis. The proteomic results showed that DMXAA had an effect on the regulation of cyclins and the cell cycle distribution at G_1/S and G_2/M DNA damage checkpoints in A549 cells with the involvement of a number of functional proteins, such as PPP2R1A, RPL5, and SKP1 (Table 2). These findings suggest that DMXAA may modulate cell cycle distribution, contributing to its anticancer effect.

Table 3 The 184 direct targets of DMXAA (5,6-dimethylxanthenone 4-acetic acid) in A549 cells analyzed by ingenuity pathway analysis

Protein ID	Symbol	Entrez gene name	Location	Type(s)	Fold change
Q5VXJ5	SYCP1	Synaptonemal complex protein 1	Nucleus	Other	−27.155
F8VVM2	SLC25A3	Solute carrier family 25 (mitochondrial carrier; phosphate carrier), member 3	Cytoplasm	Transporter	−1.762
B4DS13	EIF4B	Eukaryotic translation initiation factor 4B	Cytoplasm	Translation regulator	−1.666
E9PEU4	ARCN1	Archain 1	Cytoplasm	Other	−1.523
F5H3I4	ACTR1A	ARP1 actin-related protein 1 homolog A (yeast)	Cytoplasm	Other	−1.513
F5GY65	SLC25A11	Solute carrier family 25 (mitochondrial carrier; oxoglutarate carrier), member 11	Cytoplasm	Transporter	−1.391
F8VSA6	NEDD8	Neural precursor cell expressed, developmentally down-regulated 8	Nucleus	Enzyme	−1.352
B4DKS8	HNRNPF	Heterogeneous nuclear ribonucleoprotein F	Nucleus	Other	−1.333
F8WD96	CTSD	Cathepsin D	Cytoplasm	Peptidase	−1.289
F5GX11	PSMA1	Proteasome (prosome, macropain) subunit, α type, 1	Cytoplasm	Peptidase	−1.286
B4E1K7	STOML2	Stomatin (EPB72)-like 2	Plasma membrane	Other	−1.276
Q5TCU6	TLN1	Talin 1	Plasma membrane	Other	−1.276
F8W7P7	WDHD1	WD repeat and HMG-box DNA binding protein 1	Nucleus	Other	−1.266
E9PNH1	GANAB	α-Glucosidase; neutral AB	Cytoplasm	Enzyme	−1.250
C9JW37	PSMD14	Proteasome (prosome, macropain) 26S subunit, non-ATPase, 14	Cytoplasm	Peptidase	−1.250
B4E241	SRSF3	Serine/arginine-rich splicing factor 3	Nucleus	Other	−1.247
E9PH29	PRDX3	Peroxiredoxin 3	Cytoplasm	Enzyme	−1.245
B7Z254	PDIA6	Protein disulfide isomerase family A, member 6	Cytoplasm	Enzyme	−1.213
B4DNJ5	RPN1	Ribophorin 1	Cytoplasm	Enzyme	−1.205
D6RDN3	CPLX2	Complexin 2	Cytoplasm	Other	−1.203
E9PDQ8	SUCLG2	Succinate-CoA ligase, GDP-forming, β subunit	Cytoplasm	Enzyme	−1.200
F8W914	RTN4	Reticulon 4	Cytoplasm	Other	−1.197
F5H3T8	RARS	Arginyl-tRNA synthetase	Cytoplasm	Enzyme	−1.190
B4E0X8	FUBP1	Far upstream element (FUSE) binding protein 1	Nucleus	Transcription regulator	−1.187
F8WF81	DDB1	Damage-specific DNA binding protein 1, 127 kDa	Nucleus	Other	−1.182
B4DT43	ETFA	Electron-transfer-flavoprotein, α polypeptide	Cytoplasm	Transporter	−1.171
B4DRT4	PEBP1	Phosphatidylethanolamine binding protein 1	Cytoplasm	Other	−1.171
E9PPQ5	CHORDC1	Cysteine and histidine-rich domain (CHORD) containing 1	Other	Other	−1.164
D6RFI0	SFXN1	Sideroflexin 1	Cytoplasm	Transporter	−1.161
C9J1T2	RHOA	Ras homolog family member A	Cytoplasm	Enzyme	−1.157
C9JPV1	SLC6A6	Solute carrier family 6 (neurotransmitter transporter), member 6	Plasma membrane	Transporter	−1.150
D6RFH4	CYB5B	Cytochrome b5 type B (outer mitochondrial membrane)	Cytoplasm	Enzyme	−1.143
B4DQJ8	PGD	Phosphogluconate dehydrogenase	Cytoplasm	Enzyme	−1.115
B4E022	TKT	Transketolase	Cytoplasm	Enzyme	−1.104
G3V5P4	CFL2	Cofilin 2 (muscle)	Extracellular space	Other	−1.103
D6RF62	PAICS	Phosphoribosylaminoimidazole carboxylase, phosphoribosylaminoimidazole succinocarboxamide synthetase	Cytoplasm	Enzyme	−1.099
B3KUK2	SOD2	Superoxide dismutase 2, mitochondrial	Cytoplasm	Enzyme	−1.097

(*Continued*)

Table 3 (*Continued*)

Protein ID	Symbol	Entrez gene name	Location	Type(s)	Fold change
D6REM6	MATR3	Matrin 3	Nucleus	Other	−1.096
B7Z2V6	ATP6V1A	ATPase, H^+ transporting, lysosomal 70 kDa, V1 subunit A	Plasma membrane	Transporter	−1.091
B1AM77	STOM	Stomatin	Plasma membrane	Other	−1.087
D6RF44	HNRNPD	Heterogeneous nuclear ribonucleoprotein D	Nucleus	Transcription regulator	−1.084
B4E0R6	IPO5	Importin 5	Nucleus	Transporter	−1.079
Q5T8U3	RPL7A	Ribosomal protein L7a	Cytoplasm	Other	−1.075
A8K318	PRKCSH	Protein kinase C substrate 80K–H	Cytoplasm	Enzyme	−1.073
C8KIM0	GSR	Glutathione reductase	Cytoplasm	Enzyme	−1.072
G3V5Q1	APEX1	APEX nuclease (multifunctional DNA repair enzyme) 1	Nucleus	Enzyme	−1.071
A6NN01	H2AFV	H2A histone family, member V	Nucleus	Other	−1.071
B7Z6M1	PLS3	Plastin 3	Cytoplasm	Other	−1.071
B3KUB4	CA12	Carbonic anhydrase XII	Plasma membrane	Enzyme	−1.069
F5GWY2	ATIC	5-aminoimidazole-4-carboxamide ribonucleotide formyltransferase/inosine 5′-monophosphate cyclohydrolase	Cytoplasm	Enzyme	−1.068
B4DIT7	TGM2	Transglutaminase 2	Cytoplasm	Enzyme	−1.066
E9PRQ6	ACAT1	Acetyl-CoA acetyltransferase 1	Cytoplasm	Enzyme	−1.065
C9JPM4	ARF4	ADP-ribosylation factor 4	Cytoplasm	Other	−1.059
B1AH77	RAC2	Ras-related C3 botulinum toxin substrate 2 (rho family, small GTP binding protein Rac2)	Cytoplasm	Enzyme	−1.053
G3V3I1	PSMA6	Proteasome (prosome, macropain) subunit, α type, 6	Cytoplasm	Peptidase	−1.049
B4DVU3	EIF3C	Eukaryotic translation initiation factor 3, subunit C	Other	Translation regulator	−1.047
B4DKM5	VDAC2	Voltage-dependent anion channel 2	Cytoplasm	Ion channel	−1.045
B4DEM7	CCT8	Chaperonin containing TCP1, subunit 8 (theta)	Cytoplasm	Enzyme	−1.044
F5GX39	TMED2	Transmembrane emp24 domain trafficking protein 2	Cytoplasm	Transporter	−1.043
F5GZ27	LONP1	Lon peptidase 1, mitochondrial	Cytoplasm	Peptidase	−1.041
F5H667	ASPH	Aspartate β-hydroxylase	Cytoplasm	Enzyme	−1.040
C9JLU1	POLR2H	Polymerase (RNA) II (DNA-directed) polypeptide H	Nucleus	Enzyme	−1.040
B4DR70	FUS	Fused in sarcoma	Nucleus	Transcription regulator	−1.039
E7ETK5	IMPDH2	Inosine 5′-monophosphate dehydrogenase 2	Cytoplasm	Enzyme	−1.038
B4DXW1	ACTR3	ARP3 actin-related protein 3 homolog (yeast)	Plasma membrane	Other	−1.037
F8VNT9	CD63	CD63 molecule	Plasma membrane	Other	−1.036
E9PKZ0	RPL8	Ribosomal protein L8	Other	Other	−1.036
B7Z6A4	SURF4	Surfeit 4	Cytoplasm	Other	−1.036
F5H1S2	RPL13	Ribosomal protein L13	Cytoplasm	Other	−1.034
B4DRF4	PTPLAD1	Protein tyrosine phosphatase-like A domain containing 1	Cytoplasm	Other	−1.028
B4DZP4	DYNC1LI2	Dynein, cytoplasmic 1, light intermediate chain 2	Cytoplasm	Other	−1.024
B3KQT9	PDIA3	Protein disulfide isomerase family A, member 3	Cytoplasm	Peptidase	−1.024
E5RJR5	SKP1	S-phase kinase-associated protein 1	Nucleus	Transcription regulator	−1.024
C9JV57	BZW1	Basic leucine zipper and W2 domains 1	Cytoplasm	Translation regulator	−1.022

B4DUR8	CCT3	Chaperonin containing TCP1, subunit 3 (γ)	Cytoplasm	Other	−1.022
A8K3Z3	PSMC5	Proteasome (prosome, macropain) 26S subunit, ATPase, 5	Nucleus	Transcription regulator	−1.022
F5H8J3	CLPTM1	Cleft lip and palate associated transmembrane protein 1	Plasma membrane	Other	−1.021
B7Z4V2	HSPA9	Heat shock 70 kDa protein 9 (mortalin)	Cytoplasm	Other	−1.020
F5GY50	PTGR1	Prostaglandin reductase 1	Cytoplasm	Enzyme	−1.015
B4DPJ8	CCT6A	Chaperonin containing TCP1, subunit 6A (ζ 1)	Cytoplasm	Other	−1.014
D6RG13	RPS3A	Ribosomal protein S3A	Nucleus	Other	−1.013
C9JTK6	OLA1	Obg-like ATPase 1	Cytoplasm	Other	−1.011
F8VRG3	TWF1	Twinfilin actin-binding protein 1	Cytoplasm	Kinase	−1.007
C9JZ20	PHB	Prohibitin	Nucleus	Transcription regulator	−1.006
C9JB50	RPL28	Ribosomal protein L28	Cytoplasm	Other	−1.006
B7Z795	CES1	Carboxylesterase 1	Cytoplasm	Enzyme	−1.005
F5GYN4	OTUB1	OTU deubiquitinase, ubiquitin aldehyde binding 1	Cytoplasm	Enzyme	−1.005
B7Z4T9	CCT7	Chaperonin containing TCP1, subunit 7 (eta)	Cytoplasm	Other	−1.004
B4DGN5	GLUD1	Glutamate dehydrogenase 1	Cytoplasm	Enzyme	−1.004
B4DDF7	PPP2R1A	Protein phosphatase 2, regulatory subunit A, alpha	Cytoplasm	Phosphatase	1.002
B4DLR8	NQO1	NAD(P)H dehydrogenase, quinone 1	Cytoplasm	Enzyme	1.005
A6NLM8	SSR4	Signal sequence receptor, delta	Cytoplasm	Other	1.008
C9J7S3	DARS	Aspartyl-tRNA synthetase	Cytoplasm	Enzyme	1.009
D6RAN4	RPL9	Ribosomal protein L9	Cytoplasm	Other	1.010
B4E3C2	RPL17	Ribosomal protein L17	Cytoplasm	Other	1.012
G3V279	ERH	Enhancer of rudimentary homolog (Drosophila)	Nucleus	Other	1.017
B4DDG1	UBE2L3	Ubiquitin-conjugating enzyme E2L 3	Nucleus	Enzyme	1.020
C9JCK5	PSMA2	Proteasome (prosome, macropain) subunit, alpha type, 2	Cytoplasm	Peptidase	1.022
E9PQD7	RPS2	Ribosomal protein S2	Cytoplasm	Other	1.023
E7EX53	RPL15	Ribosomal protein L15	Cytoplasm	Other	1.024
B7ZAT2	CCT2	Chaperonin containing TCP1, subunit 2 (β)	Cytoplasm	Kinase	1.026
E9PCY7	HNRNPH1	Heterogeneous nuclear ribonucleoprotein H1 (H)	Nucleus	Other	1.026
B8ZZQ6	PTMA	α-prothymosin	Nucleus	Other	1.027
B4E335	ACTB	β-actin	Cytoplasm	Other	1.029
A6NL93	HMGN1	High mobility group nucleosome binding domain 1	Nucleus	Transcription regulator	1.029
Q5JR95	RPS8	Ribosomal protein S8	Cytoplasm	Other	1.031
C9J9K3	RPSA	Ribosomal protein SA	Cytoplasm	Translation regulator	1.031
C9JF49	XPO1	Exportin 1	Nucleus	Transporter	1.033
E9PGI8	CMPK1	Cytidine monophosphate (UMP-CMP) kinase 1, cytosolic	Nucleus	Kinase	1.034
E9PMD7	PPP1CA	Protein phosphatase 1, catalytic subunit, alpha isozyme	Cytoplasm	Phosphatase	1.035
G3V3T3	ACIN1	Apoptotic chromatin condensation inducer 1	Nucleus	Enzyme	1.038
B1ALW1	TXN	Thioredoxin	Cytoplasm	Enzyme	1.040
A8MUD9	RPL7	Ribosomal protein L7	Nucleus	Transcription regulator	1.041
Q2YDB7	PPIF	Peptidylprolyl isomerase F	Cytoplasm	Enzyme	1.042
B7Z9L0	CCT4	Chaperonin containing TCP1, subunit 4 (δ)	Cytoplasm	Other	1.045

(*Continued*)

Table 3 (*Continued*)

Protein ID	Symbol	Entrez gene name	Location	Type(s)	Fold change
E7EQR4	EZR	Ezrin	Plasma membrane	Other	1.046
F8W118	NAP1L1	Nucleosome assembly protein 1-like 1	Nucleus	Other	1.051
F8VZJ2	NACA	Nascent polypeptide-associated complex α subunit	Cytoplasm	Transcription regulator	1.055
G3V5B3	ERO1L	ERO1-like (*Saccharomyces cerevisiae*)	Cytoplasm	Enzyme	1.058
B4E2S7	LAMP2	Lysosomal-associated membrane protein 2	Plasma membrane	Enzyme	1.060
B4DR63	PSMC1	Proteasome (prosome, macropain) 26S subunit, ATPase, 1	Nucleus	Peptidase	1.060
G3V5M3	DLST	Dihydrolipoamide S-succinyltransferase	Cytoplasm	Enzyme	1.061
C9JU56	RPL31	Ribosomal protein L31	Cytoplasm	Other	1.061
B7Z1N6	ALDOC	Aldolase C, fructose-bisphosphate	Cytoplasm	Enzyme	1.062
F8VWC5	RPL18	Ribosomal protein L18	Cytoplasm	Other	1.064
C9JD32	RPL23	Ribosomal protein L23	Cytoplasm	Other	1.066
A4D177	CBX3	Chromobox homolog 3	Nucleus	Transcription regulator	1.068
Q5HYE7	CRYZ	ζ-Crystallin, (quinone reductase)	Cytoplasm	Enzyme	1.069
B4E3E8	DDX3X	DEAD (Asp-Glu-Ala-Asp) box helicase 3, X-linked	Cytoplasm	Enzyme	1.072
A8K8G0	HDGF	Hepatoma-derived growth factor	Extracellular space	Growth factor	1.074
F5H897	TRAP1	Tumor necrosis factor receptor-associated protein 1	Cytoplasm	Enzyme	1.074
E9PNR9	PRMT1	Protein arginine methyltransferase 1	Nucleus	Enzyme	1.075
E9PJH8	SERPINH1	Serpin peptidase inhibitor, clade H (heat shock protein 47), member 1	Extracellular space	Other	1.075
C9JKI3	CAV1	Caveolin 1, caveolae protein, 22 kDa	Plasma membrane	Transmembrane receptor	1.078
D6R9P3	HNRNPAB	Heterogeneous nuclear ribonucleoprotein A/B	Nucleus	Enzyme	1.081
Q8N1C0	CTNNA1	Catenin (cadherin-associated protein), α1, 102 kDa	Plasma membrane	Other	1.084
B4DY66	SAE1	SUMO1 activating enzyme subunit 1	Cytoplasm	Enzyme	1.087
F6RFD5	DSTN	Destrin (actin depolymerizing factor)	Cytoplasm	Other	1.088
C9J712	PFN2	Profilin 2	Cytoplasm	Other	1.088
F5H4D6	G3BP1	GTPase activating protein (SH3 domain) binding protein 1	Nucleus	Enzyme	1.091
B4DR31	DPYSL2	Dihydropyrimidinase-like 2	Cytoplasm	Enzyme	1.092
B6EAT9	CD44	CD44 molecule (Indian blood group)	Plasma membrane	Enzyme	1.097
B4E3S0	CORO1C	Coronin, actin binding protein, 1C	Cytoplasm	Other	1.108
C9JHS6	AKT2	V-akt murine thymoma viral oncogene homolog 2	Cytoplasm	Kinase	1.116
Q5TA01	GSTO1	Glutathione S-transferase ω1	Cytoplasm	Enzyme	1.119
F8W7C6	RPL10	Ribosomal protein L10	Cytoplasm	Other	1.124
F5H0T1	STIP1	Stress-induced phosphoprotein 1	Cytoplasm	Other	1.127
C9JFR7	CYCS	Cytochrome c, somatic	Cytoplasm	Transporter	1.128
E7EPB3	RPL14	Ribosomal protein L14	Cytoplasm	Other	1.129
F5H6Q2	UBC	Ubiquitin C	Cytoplasm	Enzyme	1.131
B4DP24	ELOVL1	ELOVL fatty acid elongase 1	Cytoplasm	Enzyme	1.135
B3KS31	TUBB6	Tubulin, β6 class V	Cytoplasm	Other	1.136
B7Z9C4	CTPS1	CTP synthase 1	Nucleus	Enzyme	1.144
F8W0G4	PCBP2	Poly(rC) binding protein 2	Nucleus	Other	1.146
F8WBE5	TFRC	Transferrin receptor	Plasma membrane	Transporter	1.147

B7Z2S5	TXNRD1	Thioredoxin reductase 1	Cytoplasm	Enzyme	1.153
B2RDM2	TXNDC5	Thioredoxin domain containing 5 (endoplasmic reticulum)	Cytoplasm	Enzyme	1.154
B4DSC0	TNPO1	Transportin 1	Nucleus	Transporter	1.155
F8VPF3	MYL6	Myosin, light chain 6, alkali, smooth muscle and non-muscle	Cytoplasm	Other	1.156
B0V3J0	TSEN34	TSEN34 tRNA splicing endonuclease subunit	Nucleus	Enzyme	1.159
F8VR50	ARPC3	Actin related protein 2/3 complex, subunit 3, 21 kDa	Cytoplasm	Other	1.162
B3KTM6	RPL5	Ribosomal protein L5	Cytoplasm	Other	1.165
Q5H907	MAGED2	Melanoma antigen family D, 2	Plasma membrane	Other	1.168
Q75MH1	RPS26	Ribosomal protein S26	Cytoplasm	Other	1.181
B4DZI8	COPB2	Coatomer protein complex, subunit beta 2 (β prime)	Cytoplasm	Transporter	1.182
Q5T4L4	RPS27	Ribosomal protein S27	Cytoplasm	Other	1.183
Q5T093	RER1	Retention in endoplasmic reticulum sorting receptor 1	Cytoplasm	Other	1.188
Q5VU59	TPM3	Tropomyosin 3	Cytoplasm	Other	1.198
Q5T7C4	HMGB1	High mobility group box 1	Nucleus	Other	1.216
C9JFK9	BAG3	Bcl2-associated athanogene 3	Cytoplasm	Other	1.219
G3V153	CAPRIN1	Cell cycle associated protein 1	Plasma membrane	Other	1.223
E5RHS5	EIF3E	Eukaryotic translation initiation factor 3, subunit E	Cytoplasm	Other	1.228
B7Z8D3	PSME3	Proteasome (prosome, macropain) activator subunit 3 (PA28 γ; Ki)	Cytoplasm	Peptidase	1.242
B4E2Z3	SLC3A2	Solute carrier family 3 (amino acid transporter heavy chain), member 2	Plasma membrane	Transporter	1.247
E9PP21	CSRP1	Cysteine and glycine-rich protein 1	Nucleus	Other	1.250
B4DMT5	EIF3F	Eukaryotic translation initiation factor 3, subunit F	Cytoplasm	Translation regulator	1.263
C9K0U8	SSBP1	Single-stranded DNA binding protein 1, mitochondrial	Cytoplasm	Other	1.271
A8MUB1	TUBA4A	α-tubulin, 4a	Cytoplasm	Other	1.298
C9IZ41	ZYX	Zyxin	Plasma membrane	Other	1.326
F5H4W0	ME1	Malic enzyme 1, $NADP^+$-dependent, cytosolic	Cytoplasm	Enzyme	1.331
B4DPJ6	TPD52L2	Tumor protein D52-like 2	Cytoplasm	Other	1.340
F5H0C8	ENO2	γ-enolase 2 (neuronal)	Cytoplasm	Enzyme	1.347
C9JL85	MTPN	Myotrophin	Nucleus	Transcription regulator	1.514
B4DPI1	PTGES3	Prostaglandin E synthase 3 (cytosolic)	Cytoplasm	Enzyme	1.801

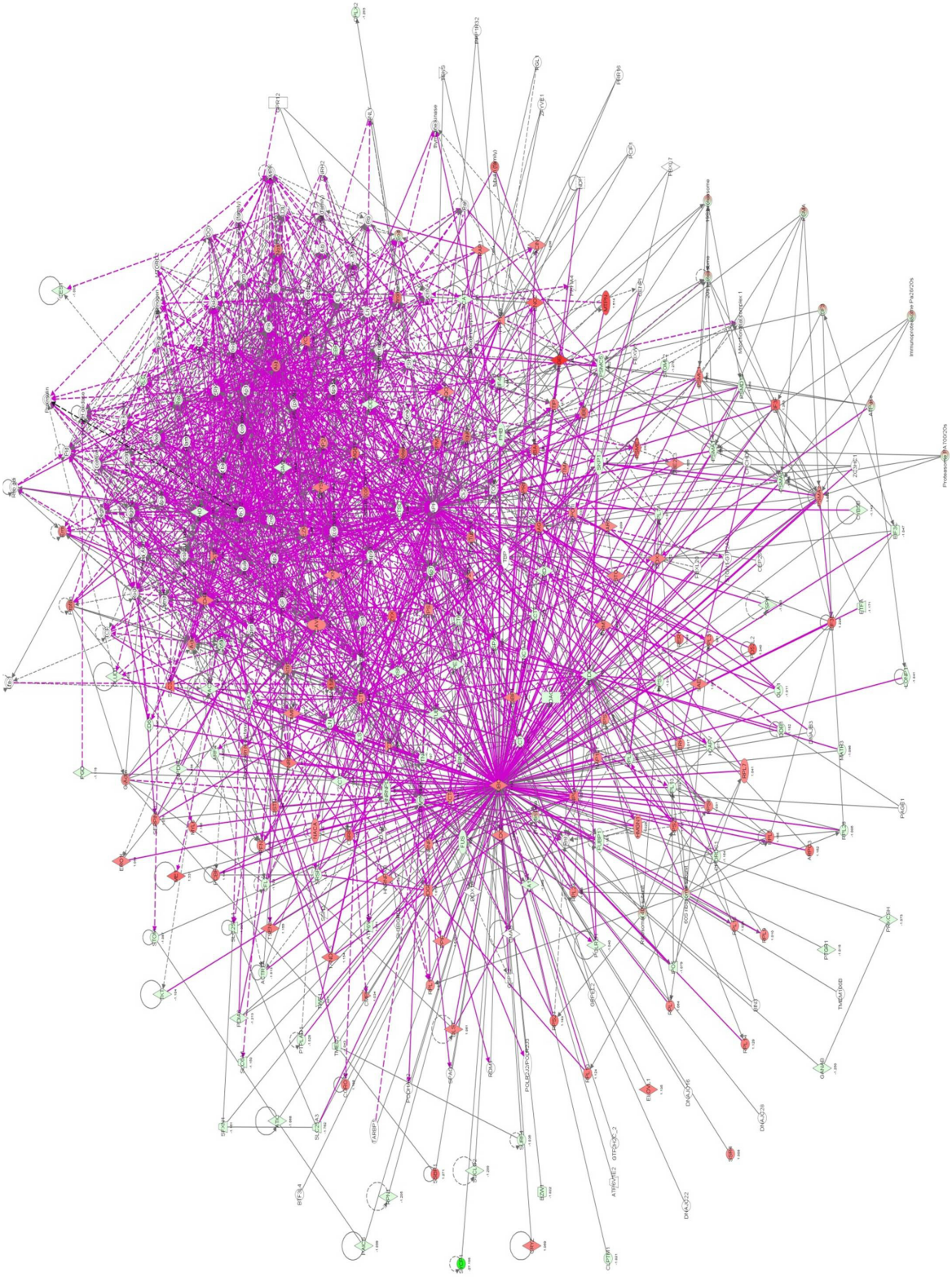

Figure 2 Proteomic analysis revealed the molecular interactome regulated by DMXAA in A549 cells.
Notes: A549 cells were treated with DMXAA 10 μM for 24 hours and the protein samples were subjected to quantitative SILAC-based proteomic analysis. There were 588 protein molecules regulated by DMXAA in A549 cells, with 281 protein molecules being increased and 306 protein molecules being decreased. Red indicates upregulation; green indicates downregulation; brown indicates predicted activation, and blue indicates predicted inhibition. The intensity of green and red molecule colors indicates the degree of downregulation and upregulation, respectively. The solid arrow indicates direct interaction and the dashed arrow indicates indirect interaction.
Abbreviations: DMXAA, 5,6-dimethylxanthenone 4-acetic acid; SILAC, stable-isotope labeling by amino acids in cell culture.

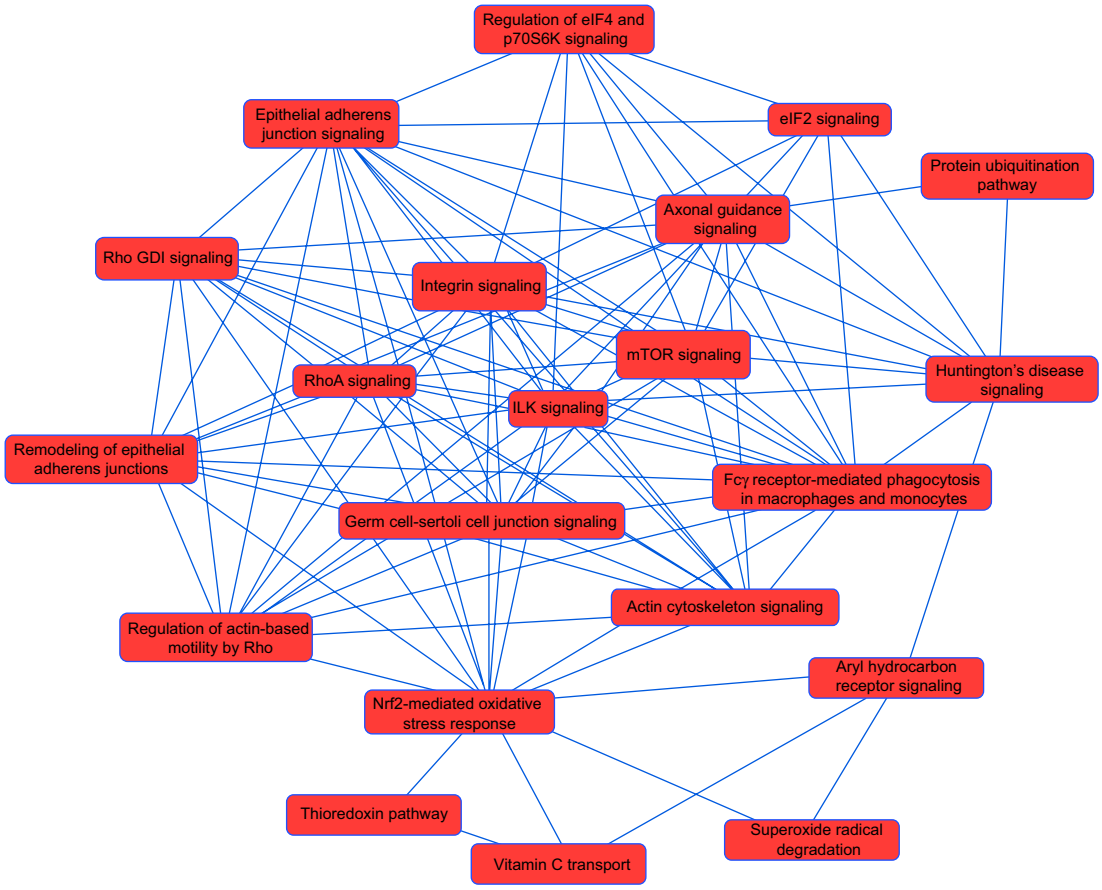

Figure 3 Proteomic analysis revealed a network of signaling pathways regulated by DMXAA in A549 cells.
Note: The network of signaling pathways was analyzed by ingenuity pathway analysis according to the 588 protein molecules regulated by DMXAA in A549 cells.
Abbreviation: DMXAA, 5,6-dimethylxanthenone 4-acetic acid; mTOR, mammalian target of rapamycin; ILK, integrin-linked kinase; Nrf2, nuclear factor erythroid 2-related factor 2; eIF, eukaryotic initiation factor; S6K, p70S6 kinase.

DMXAA regulates apoptosis and autophagy in A549 cells

Apoptosis and autophagy are two predominant programmed cell death pathways.[30] Manipulating apoptosis and autophagy has been considered to be a promising strategy in the treatment of cancer via the regulation of mitochondria-dependent/-independent pathways.[31–35] As shown in Table 2, DMXAA regulated the apoptotic signaling pathway, mitochondrial function, and death receptor signaling pathway, involving a number of functional proteins. These included ACIN1, CYCS, ACTB, AKT2, GSR, PRDX3, SOD2, and VDAC2 (Table 2). Further, the mTOR signaling pathway plays a pivotal role in the regulation of autophagy, and has been proposed to be a promising target in the treatment of NSCLC.[36] Vascular disruption combined with mTOR inhibition showed an enhanced anticancer effect when compared with monotherapy.[37] As shown in Table 2 and Figure 4, DMXAA showed an ability to modulate the mTOR signaling pathway in A549 cells. The results showed that DMXAA decreased the expression of EIF3C, EIF4B, RHOA, and RPS3A, but increased the expression of AKT2, EIF3E, EIF3F, PPP2R1A, RPS2, RPS8, RPS26, RPS27, and RPSA in A549 cells (Table 2), suggesting that modulation of mTOR signaling may play an important role in the cancer cell killing effect of DMXAA in A549 cells. Taken together, the results suggest that the regulatory effects of DMXAA on apoptosis, mitochondrial function, and mTOR signaling pathway contribute, at least in part, to the anticancer effect of this drug in the treatment of NSCLC.

DMXAA regulates redox homeostasis involving ROS-mediated and Nrf2-mediated signaling pathways in A549 cells

Induction of ROS plays a critical role in the production of cytokines, contributing to the cancer cell killing effect of DMXAA.[38] However, the regulatory effect of DMXAA on ROS generation-related molecules and signaling pathways is not fully understood. In this study, we observed that DMXAA regulated several critical signaling pathways related to ROS generation and redox homeostasis in A549 cells.

Table 4 Networks of potential molecular targets regulated by DMXAA (5,6-dimethylxanthenone 4-acetic acid) in A549 cells

ID	Molecules in network	Score	Focus molecules	Top diseases and functions
1	ASPH, ATIC, BZW1, CHORDC1, CLPTM1, CMPK1, CRYZ, CYB5B, DYNC1LI2, ELOVL1, GANAB, H2AFV, ME1, OLA1, PAICS, PDIA6, PGD, PRKCSH, PTGR1, RER1, SAE1, SFXN1, SLC25A3, SLC25A11, SLC6A6, SSBP1, STOM, SUCLG2, SURF4, SYCP1, TMED2, TPD52L2, TSEN34, TXNDC5, UBC	77	35	Carbohydrate metabolism, small molecule biochemistry, lipid metabolism
2	60S ribosomal subunit, ACIN1, Akt, CD63, DDX3X, EIF3, EIF3C, EIF3E, EIF3F, EIF4B, histone H1, HNRNPF, β-importin, IPO5, MTORC2, NEDD8, Rar, RPL5, RPL7, RPL9, RPL10, RPL13, RPL14, RPL15, RPL17, RPL18, RPL23, RPL28, RPL31, RPL7A, SLC3A2, thymidine kinase, TNPO1, TPM3, TRAP1	52	27	Gene expression, protein synthesis, cancer
3	APEX1, ARF4, ARPC3, collagen type I, cytochrome C, ERK, ETFA, HDGF, HISTONE, HMGB1, HMGN1, HNRNPD, Hsp27, mitochondrial complex 1, NACA, NAP1L1, PHB, PLS3, PP2A, PPP2R1A, PRDX3, PRMT1, PTMA, ribosomal 40s subunit, RNR, RPS2, RPS8, RPS26, RPS27, RPS3A, RPSA, STOML2, TCF, VDAC2, XPO1	47	25	Cellular response to therapeutics, connective tissue development and function, carbohydrate metabolism
4	19S proteasome, 20s proteasome, 26s proteasome, α-tubulin, ATPase, BAG3, β-tubulin, CCT2, CCT3, CCT4, CCT7, CCT8, CCT6A, FUBP1, GSR, IκB, immunoproteasome Pa28/20s, LAMP2, LONP1, MTPN, NF-κB (complex), NQO1, PEBP1, proteasome PA700/20s, PSMA, PSMA1, PSMA2, PSMA6, PSMC1, PSMC5, PSMD14, PSME3, PTPLAD1, TUBB6, ubiquitin	41	23	Cell death and survival, DNA replication, recombination, and repair, energy production
5	ACTB, actin, ACTR1A, α-actinin, CAPRIN1, CFL2, cofilin, DARS, DLST, DPYSL2, DSTN, ERK1/2, Erm, EZR, F-actin, gilamin, G-actin, G3BP1, GLUD1, Na^+, K^+-ATPase, PCBP2, PFN2, PKG, profilin, proinsulin, Rho GDI, Rock, RPL8, RTN4, SRSF3, thioredoxin reductase, TLN1, TWF1, TXNRD1, ZYX	34	20	Cellular assembly and organization, cellular compromise, cellular function and maintenance
6	ALDOC, ATP6V1A, ATP6V1E2, BIN3, BTF3L4, CORO1C, DDB1, DNAJB3, DNAJC16, DNAJC22, DNAJC28, ERH, GRPEL2, GTF2H2C_2, HNRNPAB, HNRNPH1, HSPA9, MATR3, OTUB1, PAGE1, PCDHAC2, POLR2H, POLR2J2/POLR2J3, PPIF, RDM1, RPN1, SERPINH1, SPAG7, SSR4, STON1-GTF2A1L, TARBP1, TBP, TMEM106B, tubulin (complex), UBC	25	16	Gene expression, cell morphology, cellular assembly and organization
7	ACAT1, ADCY, AMPK, CA12, calmodulin, caspase, CK2, Creb, CSRP1, CTSD, cyclin A, CYCS, ERO1L, estrogen receptor, FUS, Hsp70, Hsp90, IL1, IMPDH2, insulin, Lh, MYL6, NOS, PDIA3, PI3K (complex), PLC, PTGES3, Rb, RNA polymerase II, STIP1, TGM2, thyroid hormone receptor, TUBA4A, tubulin (family), TXN	23	15	Neurological disease, skeletal and muscular disorders, cell death and survival
8	ACTR3, α-catenin, ARCN1, CBX3, CD3, COPB2, CTNNA1, CTPS1, hemoglobin, histone H3, histone H4, IFN-β, IgG, IL12 (complex), immunoglobulin, interferon-α, MAGED2, MAPK, mediator, NMDA receptor, p38 MAPK, PKA, PKC(s), PLC-γ, RARS, Ras homolog, SFK, SRC (family), STAT5a/b, TFRC, TNF (family), trypsin, VEGF, WDHD1	14	10	Infectious disease, cardiac damage, cardiac fibrosis
9	AKT2, AP1, BCR (complex), calpain, CAV1, CD44, collagen(s), ENO2, fibrinogen, focal adhesion kinase, IGM, integrin, JNK, laminin, LDH (complex), LDL, LFA-1, MEK, NADPH oxidase, NFAT (family), p85 (PI3K), PDGF (complex), PDGF BB, PI3K (family), Pld, Rac, RAC2, Ras, RHOA, SOD, SOD2, SOS, TGF-β, TKT, tyrosine kinase	10	8	Free radical scavenging, cell morphology, cellular assembly and organization
10	APP, CENPI, CEP250, CES1, CHCHD6, CMAS, CPLX2, DDX10, ERBB2, FBXL7, FBXL20, FBXW9, FSH, GNLY, GNRH2, GPR12, GSK3, GSPT2, GSTO1, MTORC1, NDP, PCIF1, PDXP, PPFIA4, PPP1CA, PPP1R32, PRR16, RGL1, SH3BGRL3, SKP1, SSH3, TSKS, UBE2L3, ZC3HC1, ZFYVE1	7	6	Cell morphology, cellular function and maintenance, cardiovascular system development and function

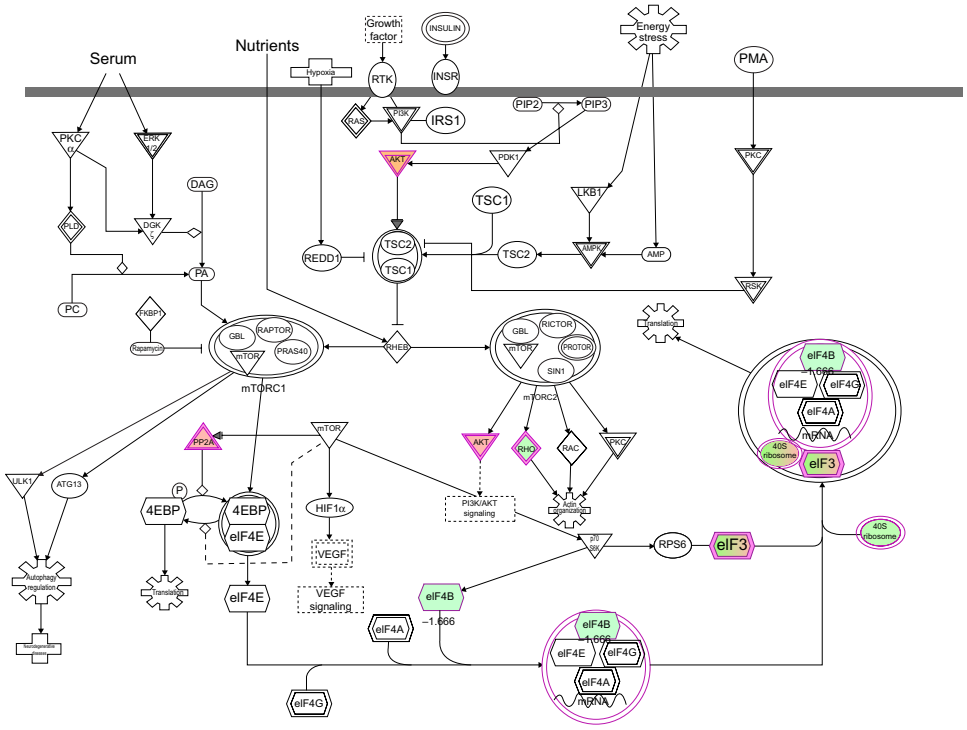

Figure 4 DMXAA modulates mTOR signaling pathway in A549 cells.

Notes: A549 cells were treated with DMXAA 10 μM for 24 hours and the protein samples were subject to quantitative proteomic analysis. Red indicates upregulation; green indicates downregulation; brown indicates predicted activation. The intensity of green and red molecule colors indicates the degree of downregulation and upregulation, respectively. The solid arrow indicates direct interaction and the dashed arrow indicates indirect interaction.

Abbreviations: DMXAA, 5,6-dimethylxanthenone 4-acetic acid; mTOR, mammalian target of rapamycin; eIF, eukaryotic initiation factor; AKT, protein kinase B; PKC, protein kinase C; TSC, tuberous sclerosis complex; VEGF, vascular endothelial growth factor; HIF, hypoxia-inducible factor; DAG, diacylglycerol; ATG, autophagy-associated protein; PMA, phorbol myristate acetate; PIP2, phosphatidylinositol 4,5-bisphosphate; IRS1, insulin receptor substrate-1; RTK, receptor tyrosine kinase; LKB1, liver kinase B1; REDD1, protein regulated in development and DNA damage response 1; PI3K, phosphatidylinositide 3-kinase; 4EBP, eukaryotic translation initiation factor 4E binding protein 1; INSR, insulin receptor; AMPK, AMP-activated protein kinase.

Our quantitative proteomic study showed that treatment with DMXAA regulated oxidative phosphorylation, Nrf2-mediated oxidative stress response, and superoxide radical degradation in A549 cells (Table 2 and Figure 5). A number of functional proteins were found to be involved in these pathways, including ACTB, CCT7, GSR, GSTO1, NQO1, PTPLAD1, SOD2, STIP1, TXN, and TXNRD1 (Table 2). Of note, Nrf2-mediated signaling pathways have a critical role in the maintenance of intracellular redox homeostasis in response to various stimuli via regulating antioxidant responsive elements.[39,40] The quantitative proteomic data suggest that modulation of the expression of functional proteins involved in Nrf2-mediated signaling pathways may contribute to the anticancer effect of DMXAA in the treatment of NSCLC.

Taken together, our quantitative proteomic study revealed a number of important functional proteins and associated signaling pathways that are regulated in A549 cells in response to treatment with DMXAA. These cellular signaling pathways play a pivotal role in the regulation of the cell cycle, apoptosis, autophagy, and oxidative stress. In our subsequent validation experiments, we confirmed the effect of DMXAA on cell cycle distribution, apoptosis, autophagy, and ROS generation in A549 cells.

Verification of molecular targets of DMXAA in A549 cells

The quantitative proteomic studies described above showed that DMXAA can modulate a number of functional protein molecules and related signaling pathways involved in cell proliferation, invasion and migration, death, and survival. In order to verify the quantitative proteomic data further, we investigated how DMXAA affected cell cycle distribution, apoptosis, autophagy, and redox homeostasis in A549 cells.

DMXAA induces G_1 arrest in A549 cells

To validate the effect of DMXAA on cell growth, the cell cycle distribution was determined in A549 cells using flow cytometric analysis. As shown in Figure 6, a concentration-dependent increase in the cell number in G_1 phase was observed after incubation of A549 cells with DMXAA at 0.1, 1, and 10 μM for 24 hours, with a 1.1-fold, 1.1-fold, and 1.4-fold increase in the number of cells arrested in G_1 phase, respectively, compared

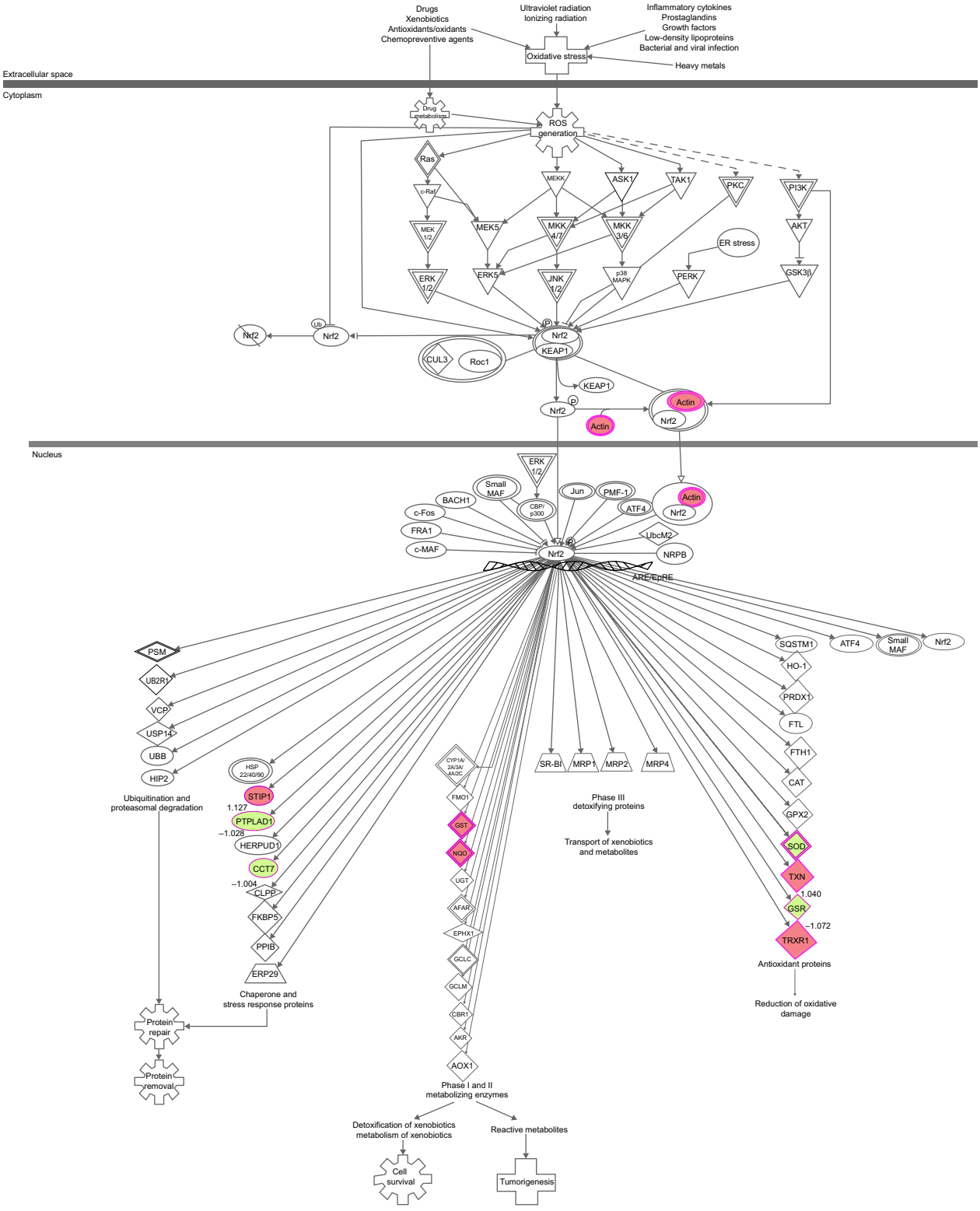

Figure 5 DMXAA regulates Nrf2-mediated signaling pathways in A549 cells.

Notes: A549 cells were treated with DMXAA 10 μM for 24 hours and the protein samples were subjected to quantitative proteomic analysis. Red indicates upregulation and green indicates downregulation. The intensity of green and red molecule colors indicates the degree of downregulation and upregulation, respectively. The solid arrow indicates direct interaction and the dashed arrow indicates indirect interaction.

Abbreviation: DMXAA, 5,6-dimethylxanthenone 4-acetic acid; ER, endoplasmic reticulum; ROS, reactive oxygen species; Nrf2, nuclear factor erythroid 2-related factor 2; SOD, superoxide dismutase; HO-1, heme oxygenase 1; GST, glutathione *S*-transferase; UGT, uridine 5'-diphospho-glucuronosyltransferase; CCT7, chaperonin containing TCP1, subunit 7; CAT, catalase; FMO, flavin-containing monooxygenase; MRP, multi-drug resistance associated protein; PSM, proteasome; VCP, valosin containing protein; UBB, ubiquitin B; HIP2, huntingtin interacting protein 2; TXN, thioredoxin; FTL, ferritin, light polypeptide; ATF4, activating transcription factor 4; BACH1, BTB and CNC homology 1, basic leucine zipper transcription factor 1; ERK, extracellular signal-regulated kinase; HSP, heat shock protein; PMF-1, polyamine-modulated factor 1; NRPB, nuclear restricted protein, BTB domain-like; MAF, v-maf avian musculoaponeurotic fibrosarcoma oncogene homolog; CYP, cytochrome P450; KEAP1, Kelch-like ECH-associated protein 1; MEK2, MAP kinase kinase 2; ASK1, apoptosis signal regulating kinase 1; TAK1, testicular receptor 4; GSK3, glycogen synthase kinase 3; JNK, c-Jun N-terminal kinase 1; CUL3, cullin 3; MEKK, MAP kinase kinase kinase.

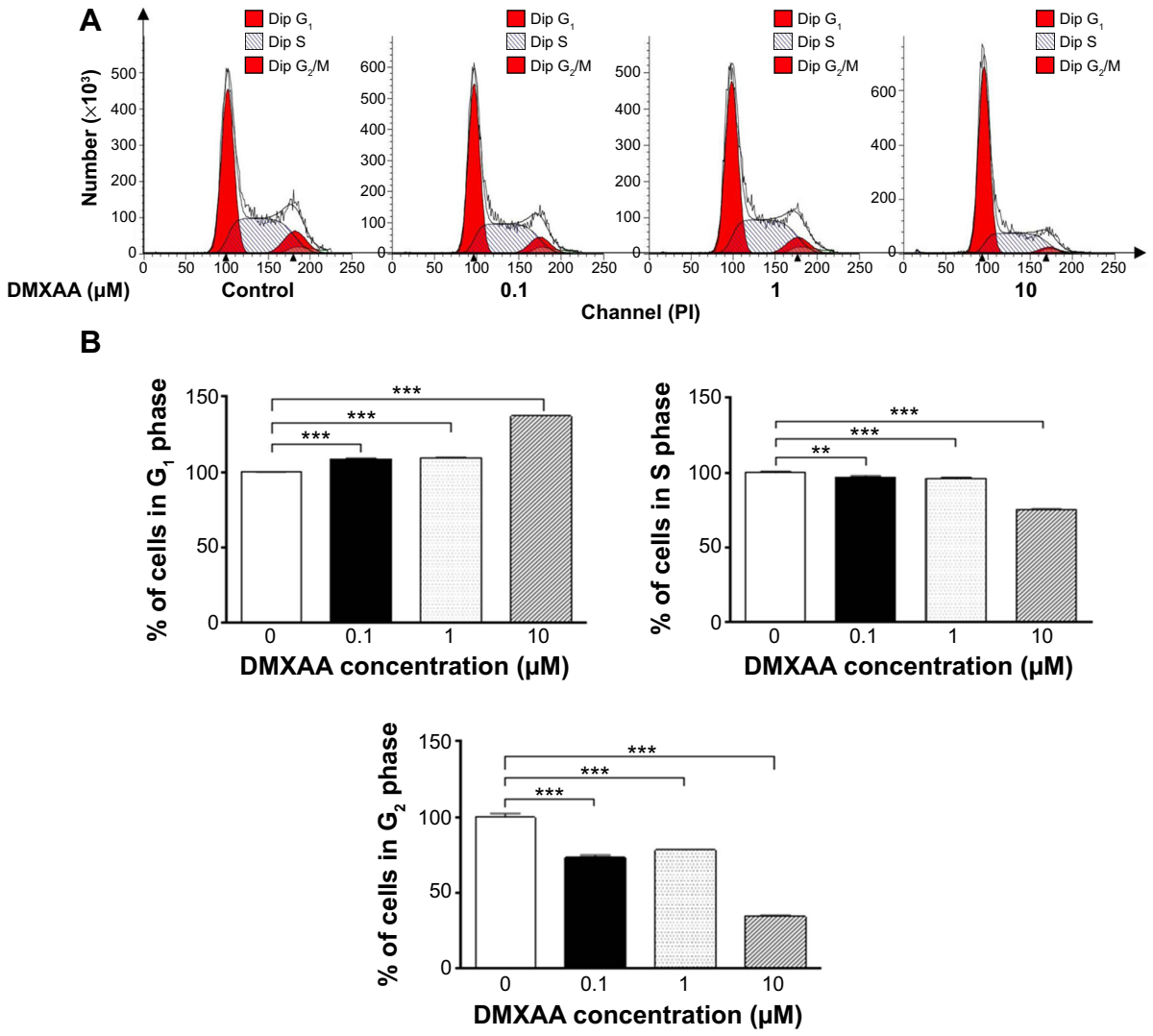

Figure 6 DMXAA induces G_1 phase arrest in A549 cells.
Notes: Cell cycle distribution of A549 cells when treated with DMXAA 0.1, 1, or 0 μM for 24 hours. (**A**) Representative DNA fluorescence histograms showing the effect of DMXAA on cell cycle distribution of A549 cells and (**B**) bar graphs showing the percentage of A549 cells in G_1, S, and G_2 phases. Data are shown as the mean ± SD of three independent experiments. $^{**}P<0.01$ and $^{***}P<0.001$ by one-way analysis of variance.
Abbreviation: DMXAA, 5,6-dimethylxanthenone 4-acetic acid.

with control cells treated with vehicle only ($P<0.001$ by one-way ANOVA, Figure 6A and B). In contrast, there was a marked decrease in the number of cells in S and G_2/M phases in A549 cells treated with DMXAA at 0.1, 1, and 10 μM for 24 hours ($P<0.01$ or $P<0.001$ by one-way ANOVA, Figure 6A and B). Taken together, the results show that DMXAA can regulate the cell cycle distribution, contributing to its anticancer effect in A549 cells. Moreover, the inducing effect of DMXAA on cell cycle arrest further verifies the regulatory action of DMXAA on G_1 and G_2 checkpoints as determined by our proteomic study.

DMXAA induces apoptosis and autophagy in A549 cells

As stated in our proteomic results, treatment with DMXAA induced apoptotic and autophagic responses in A549 cells involving several important signaling pathways. In the mitochondria/cytochrome c-mediated apoptotic pathway, release of cytochrome c from the mitochondria to the cytosol and resultant activation of the caspase cascade are key steps in the apoptosis process.[41,42] Beclin 1 and LC3-I/II are two important markers in the initiation and progression of autophagy and are critical for formation of autophagosomes.[43,44] During the autophagy process, LC3/Atg8 is cleaved at its C-terminus by Atg4 to generate cytosolic LC3-I.[45] LC3-I is subsequently conjugated to phosphatidylethanolamine, then proteolytically cleaved and lipidated by Atg3 and Atg7 to form LC3-II, which attaches to the membrane of the autophagosome.

To verify the proteomic response to DMXAA with regard to cell death, we performed Western blotting assays to

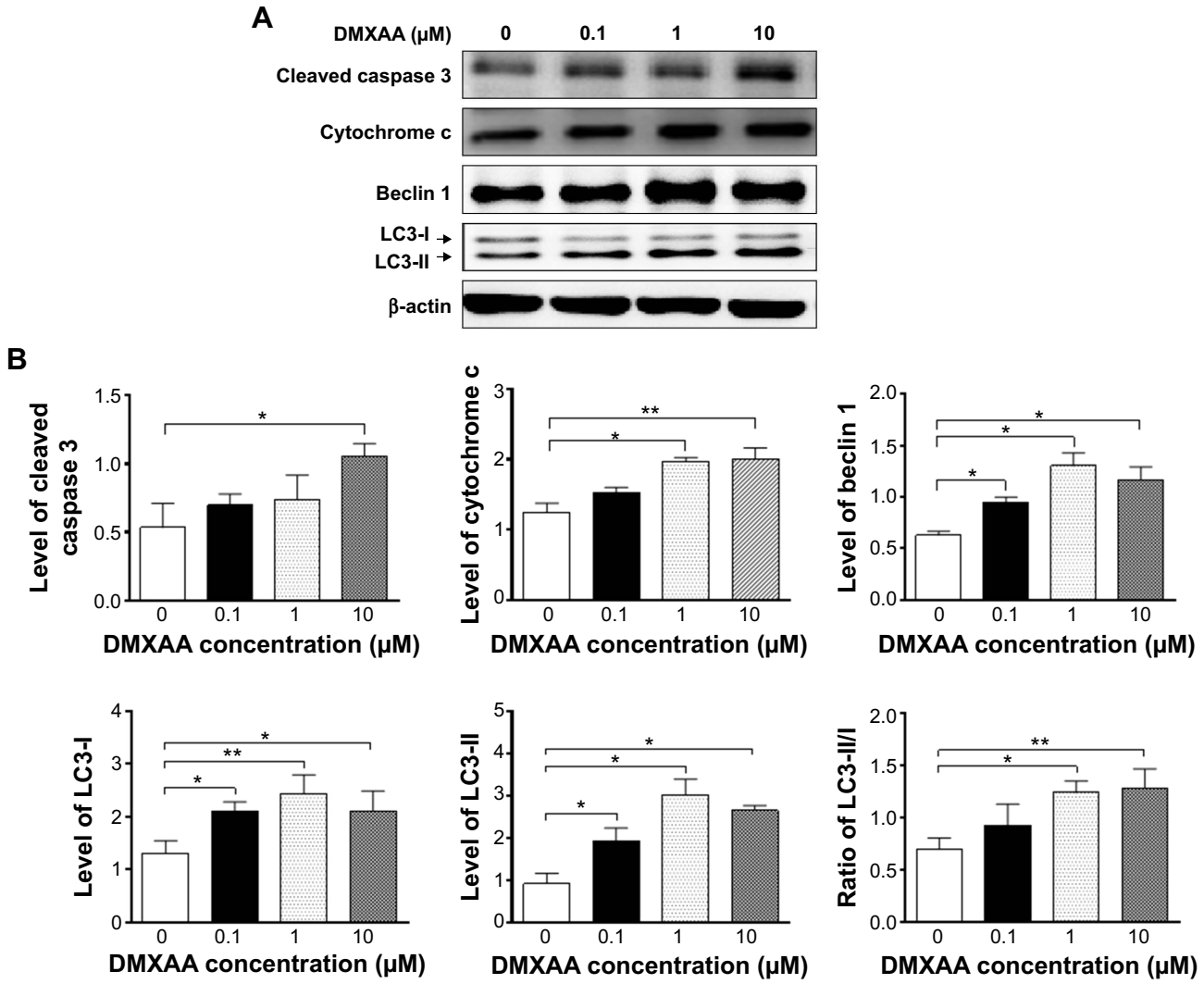

Figure 7 DMXAA increases the cytosolic level of cytochrome c and activation of caspase 3, and promotes expression of beclin 1, LC3-I, and LC3-II in A549 cells.
Notes: A549 cells were treated with DMXAA 0.1, 1, or 10 μM for 24 hours and protein samples were subjected to Western blotting assay. (**A**) Representative blots of cytosolic cytochrome c, cleaved caspase 3, beclin 1, LC3-I, and LC3-II in A549 cells and (**B**) bar graphs showing the relative levels of cytosolic cytochrome c, cleaved caspase 3, beclin 1, LC3-I, and LC3-II in A549 cells. Data are shown as the mean ± SD of three independent experiments. *$P<0.05$ and **$P<0.01$ by one-way analysis of variance.
Abbreviations: DMXAA, 5,6-dimethylxanthenone 4-acetic acid; LC3, microtubule-associated protein 1A/1B-light chain 3.

examine the expression of cytochrome c, caspase 3, beclin 1, and LC3-I/II in A549 cells treated with DMXAA. Incubation of A549 cells with DMXAA at 0.1, 1, and 10 μM markedly increased the cytosolic level of cytochrome c by 1.2-, 1.6-, and 1.6-fold, respectively, compared with the control cells ($P<0.05$ or $P<0.01$ by one-way ANOVA, Figure 7A and B). Cleaved caspase 3 was increased by DMXAA in A549 cells in a concentration-dependent manner. Incubation of A549 cells with DMXAA at 0.1, 1, and 10 μM significantly increased the level of cleaved caspase 3 by 1.3-, 1.4-, and 2.0-fold, respectively, compared with control cells ($P<0.05$ by one-way ANOVA, Figure 7A and B). These results indicate that DMXAA induces a marked increase in the cytosolic level of cytochrome c and activation of caspase 3, eventually leading to apoptotic death in A549 cells.

We further examined the effect of DMXAA on beclin 1 and LC3-I/II expression levels. Treatment of A549 cells with DMXAA for 24 hours significantly increased the expression of beclin 1. There was a 1.5-, 2.1-, and 1.9-fold increase in beclin 1 in A549 cells treated with DMXAA 0.1, 1, and 10 μM, respectively, for 24 hours ($P<0.05$ by one-way ANOVA, Figure 7A and B). Upon activation of LC3-I/II, our Western blotting analysis revealed two clear bands of LC3-I and II in A549 cells after 24 hour treatment with DMXAA (Figure 7A). Incubation of DMXAA at 0.1, 1, and 10 μM markedly increased the expression of LC3-I and LC3-II (Figure 7A and B). In comparison with the control cells, there was a 1.6-, 1.9-, and 1.6-fold increase in the level of LC3-I, and a 2.1-, 3.3-, and 2.9-fold increase in the level of LC3-II in A549 cells treated with DMXAA 0.1, 1, and 10 μM, respectively,

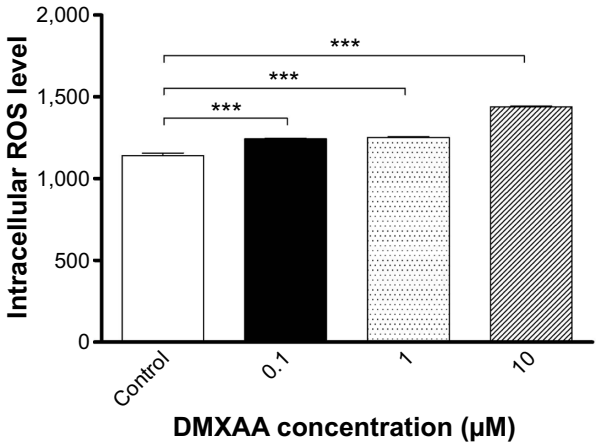

Figure 8 DMXAA induces intracellular ROS generation in A549 cells.
Notes: Intracellular ROS level in A549 cells treated with DMXAA 0.1, 1, or 10 μM for 48 hours. Data are shown as the mean ± SD of three independent experiments. ***$P<0.01$ by one-way analysis of variance.
Abbreviation: DMXAA, 5,6-dimethylxanthenone 4-acetic acid; ROS, reactive oxygen species.

for 24 hours. In addition, the ratio of LC3-II to LC3-I was markedly increased by 1.3-, 1.8-, and 1.8-fold in A549 cells treated with DMXAA 0.1, 1, and 5 μM, respectively ($P<0.05$ or $P<0.01$ by one-way ANOVA, Figure 7A and B). Taken together, the proteomic and Western blotting results show that DMXAA induces apoptosis and autophagy in A549 cells, contributing to the anticancer effects of DMXAA in the treatment of NSCLC.

DMXAA induces generation of intracellular ROS in A549 cells

As shown in the proteomic results, treatment with DMXAA can regulate intracellular redox homeostasis in A549 cells, which may contribute to the apoptosis-inducing and autophagy-inducing effects of DMXAA. Thus, we determined the effect of DMXAA on intracellular ROS levels in A549 cells. The intracellular levels of ROS were increased 1.1-, 1.1-, and 1.3-fold in a concentration-dependent manner when A549 cells were treated with DMXAA 0.1, 1, and 10 μM for 48 hours ($P<0.001$ by one-way ANOVA, Figure 8). The ROS-inducing effect of DMXAA further confirms its regulatory effect on intracellular redox homeostasis in A549 cells.

Discussion

NSCLC remains a devastating cancer, with the highest incidence and mortality rate, and treatment of the disease remains a major challenge due to the poor efficacy and severe side effects of both standard and new chemotherapeutic agents. There is an increasing interest in new agents and therapies for the treatment of lung cancer. DMXAA, a flavonoid tumor vascular-disrupting agent, has been found to have anticancer activity in vitro and in vivo in the treatment of NSCLC when used alone or in combination. It targets the established tumor blood vessels and inhibits tumor blood flow, resulting in necrosis of solid tumors. It has also been reported that DMXAA can regulate multiple signaling pathways involved in cell cycle progression, apoptosis, autophagy, and ROS generation.[11,46–51] However, the global potential molecular targets and the possible mechanisms involved are not fully identified as yet. In the present study, we showed a comprehensive network of signaling pathways responding to treatment with DMXAA in A549 cells using a quantitative SILAC-based proteomic approach. The network of signaling pathways was mainly involved in cell cycle distribution, cell invasion and migration, redox homeostasis, and cell death. We verified that DMXAA arrested A549 cells in G_1 phase, promoted apoptosis, induced marked autophagy, and triggered ROS generation.

The SILAC-based proteomic approach can quantitatively and comprehensively evaluate the effect of a given compound and identify its potential molecular targets and related signaling pathways.[52–54] Previous studies have used this approach in A549 cells and tried to explore the potential molecular targets and possible mechanism for NSCLC therapy.[55–63] In our study, we used a quantitative SILAC-based proteomic approach to evaluate the responses of A549 cells to treatment with DMXAA. This approach showed that DMXAA regulates a number of functional proteins and molecular signaling pathways involved in cell cycle progression, apoptosis, autophagy, and redox homeostasis in A549 cells, such as PPP2R1A, RPL5, SKP1, ACIN1, CYCS, ACTB, AKT2, GSR, PRDX3, SOD2, VDAC2, EIF3C, EIF4B, RHOA, RPS3A, AKT2, EIF3E, EIF3F, PPP2R1A, RPS2, RPS8, RPS26, RPS27, RPSA, ACTB, CCT7, GSR, GSTO1, NQO1, PTPLAD1, STIP1, TXN, and TXNRD1. The proteomic results suggest that DMXAA may target these molecules to elicit its anticancer effects in the treatment of NSCLC. Notably, we went on to validate the proteomic responses to DMXAA in A549 cells.

We found that DMXAA arrested A549 cells in G_1 phase in a concentration-dependent manner, and speculated that the possible mechanism of DMXAA with regard to G_1 arrest in A549 cells might involve a number of key regulators, including p21 Waf1/Cip1, p53, cyclins and cyclin-dependent kinases. p21 is a cyclin-dependent kinase inhibitor regulated by p53, and can bind to the Cdc2-cyclin B1 complex, thereby inducing cell cycle arrest.[64] Further, cell cycle progression is tightly regulated by cyclins and cyclin-dependent kinases.[65] Cyclins have no catalytic activity and are inactive in the

absence of a partner cyclin. The complex formed by the association of Cdc2 and cyclin B1 plays a major role in the entry of cells into mitosis. Phosphorylation of Cdc2 at Thr161 by cyclin-dependent kinase–activating kinases is essential for the activity of Cdc2 kinase. Phosphorylation of Cdc2 at Thr14 and Tyr15 is catalyzed by Wee1 and Myt1 protein kinases, resulting in inhibition of Cdc2.[65] During G_2/M transition, Cdc2 is rapidly converted into the active form by dephosphorylation of Tyr14 and Tyr15, catalyzed by Cdc25 phosphatase. Thus, taking the proteomic and flow cytometric results into consideration, DMXAA-induced cell cycle arrest may occur via regulation of key modulators controlling the G_1 and G_2 checkpoints in A549 cells.

The present proteomic study also shows that DMXAA regulated mitochondrial function and cell death. Mitochondrial disruption and subsequent release of cytochrome c initiates the process of apoptosis, with the latter being initiated by proapoptotic members of the Bcl-2 family but antagonized by antiapoptotic members of this family.[66,67] Antiapoptotic members of Bcl-2 can be inhibited by post-translational modification and/or by increased expression of PUMA, which is an essential regulator of p53-mediated cell apoptosis.[68] In addition, cytochrome c released from the mitochondria can activate caspase 9, which then activates caspase 3 and caspase 7.[69] In our study, we observed that the cytosolic level of cytochrome c was significantly increased and that caspase 3 was markedly activated after treatment with DMXAA. The activated caspase 3 ultimately induced apoptosis, with a decrease in the Bcl-2 level.

Further, the proteomic results show that DMXAA has a modulating effect on the mTOR signaling pathway. Under optimal growth conditions, activated mTORC1 inhibits autophagy by direct phosphorylation of Atg13 and ULK1 at Ser757.[70–72] This phosphorylation inhibits ULK1 kinase activity and subsequent autophagosome formation. When the kinase activity of mTORC1 is suppressed, the autophagic machinery is initiated. In the present study, DMXAA induced autophagy in A549 cells as indicated by the increased expression of beclin 1 and the ratio of LC3-II over LC3-I. The amount of LC3-II or the ratio between LC3-II and LC3-I correlates well with the number of autophagosomes. Taken together, the autophagy-inducing effect of DMXAA may contribute to its anticancer activity via regulation of the mTOR signaling pathway.

In addition, our proteomic study showed that DMXAA regulates the Nrf2-mediated signaling pathway, which controls the basal and induced expression of a wide array of antioxidant response element-dependent genes to regulate the physiological and pathophysiological outcomes of exposure to oxidants.[40,73,74] We found a significant inducing effect of DMXAA on ROS generation in A549 cells. However, the mechanism of how DMXAA induces ROS generation is unclear. Nrf2 is a nuclear transcription factor that plays a pivotal role in regulation of oxidative stress by modulating the transcription of antioxidant response elements.[40] It indicates that DMXAA may induce oxidative stress via the Nrf2-mediated signaling pathway. Our results suggest that ROS may have an important role in DMXAA-induced apoptosis and autophagy in A549 cells. However, further studies are needed to elucidate how DMXAA induces generation of ROS and modulates redox homeostasis.

In summary, the quantitative SILAC-based proteomic approach used in this study showed that DMXAA inhibited cell proliferation, predominantly activated the mitochondria-dependent apoptotic pathway and induced autophagy, and increased intracellular levels of ROS in human A549 cells involving a number of key functional proteins and related molecular signaling pathways. This study may provide a clue enabling full identification of the molecular targets and elucidate the underlying mechanisms of DMXAA in the treatment of NSCLC, resulting in an improved therapeutic effect and fewer side effects in the clinical setting.

Acknowledgments

The authors appreciate the financial support of the Startup Fund of the College of Pharmacy, University of South Florida, Tampa, FL, USA. Dr Zhi-Wei Zhou, PhD, holds a postdoctoral scholarship from the College of Pharmacy, University of South Florida.

Disclosure

The authors report no conflicts of interest in this work.

References

1. Siegel R, Desantis C, Jemal A. Cancer statistics, 2014. *CA Cancer J Clin*. 2014;64(1):9–29.
2. Ferlay J, Soerjomataram I, Ervik M, et al. GLOBOCAN 2012 v1.0, Cancer Incidence and Mortality Worldwide: IARC CancerBase No. 11. Lyon, France: International Agency for Research on Cancer; 2013. Available from: http://globocan.iarc.fr. Accessed December 10, 2014.
3. US Cancer Statistics Working Group. United States Cancer Statistics: 1999–2011 Incidence and Mortality Web-based Report. Atlanta, GA, USA: Department of Health and Human Services, Centers for Disease Control and Prevention, National Cancer Institute; 2014. Available from: http://www.cdc.gov/cancer/npcr/pdf/USCS_FactSheet.pdf. Accessed December 10, 2014.
4. American Cancer Society. Cancer Facts and Figures 2014. Atlanta, GA, USA: American Cancer Society; 2014. Available from: http://www.cancer.org/research/cancerfactsstatistics/cancerfactsfigures2014/. Accessed December 10, 2014.

5. Wang YC, Wei LJ, Liu JT, Li SX, Wang QS. Comparison of Cancer Incidence between China and the USA. *Cancer Biol Med*. 2012;9(2):128–32.
6. Keith RL, Miller YE. Lung cancer chemoprevention: current status and future prospects. *Nat Rev Clin Oncol*. 2013;10(6):334–343.
7. Siegel R, Naishadham D, Jemal A. Cancer statistics, 2012. *CA Cancer J Clin*. 2012;62(1):10–29.
8. Brown SL, Kolozsvary A, Kim JH. Vascular targeting therapies for treatment of malignant disease. *Cancer*. 2005;104(1):216–217.
9. Amir E, Mandoky L, Blackhall F, et al. Antivascular agents for non-small-cell lung cancer: current status and future directions. *Expert Opin Investig Drugs*. 2009;18(11):1667–1686.
10. Zhou S, Kestell P, Baguley BC, Paxton JW. 5,6-Dimethylxanthenone-4-acetic acid (DMXAA): a new biological response modifier for cancer therapy. *Invest New Drugs*. 2002;20(3):281–295.
11. Buchanan CM, Shih JH, Astin JW, et al. DMXAA (vadimezan, ASA404) is a multi-kinase inhibitor targeting VEGFR2 in particular. *Clin Sci (Lond)*. 2012;122(10):449–457.
12. Li J, Jameson MB, Baguley BC, Pili R, Baker SD. Population pharmacokinetic-pharmacodynamic model of the vascular-disrupting agent 5,6-dimethylxanthenone-4-acetic acid in cancer patients. *Clin Cancer Res*. 2008;14(7):2102–2110.
13. Zhou S, Paxton JW, Tingle MD, Kestell P. Identification of the human liver cytochrome P450 isoenzyme responsible for the 6-methylhydroxylation of the novel anticancer drug 5,6-dimethylxanthenone-4-acetic acid. *Drug Metab Dispos*. 2000;28(12):1449–1456.
14. Miners JO, Valente L, Lillywhite KJ, et al. Preclinical prediction of factors influencing the elimination of 5,6-dimethylxanthenone-4-acetic acid, a new anticancer drug. *Cancer Res*. 1997;57(2):284–289.
15. McKeage MJ, Von Pawel J, Reck M, et al. Randomised phase II study of ASA404 combined with carboplatin and paclitaxel in previously untreated advanced non-small cell lung cancer. *Br J Cancer*. 2008;99(12):2006–2012.
16. Lara PN Jr, Douillard JY, Nakagawa K, et al. Randomized phase III placebo-controlled trial of carboplatin and paclitaxel with or without the vascular disrupting agent vadimezan (ASA404) in advanced non-small-cell lung cancer. *J Clin Oncol*. 2011;29(22):2965–2971.
17. Pili R, Rosenthal MA, Mainwaring PN, et al. Phase II study on the addition of ASA404 (vadimezan; 5,6-dimethylxanthenone-4-acetic acid) to docetaxel in CRMPC. *Clin Cancer Res*. 2010;16(10):2906–2914.
18. Fruh M, Cathomas R, Siano M, et al. Carboplatin and paclitaxel plus ASA404 as first-line chemotherapy for extensive-stage small-cell lung cancer: a multicenter single arm phase II trial (SAKK 15/08). *Clin Lung Cancer*. 2013;14(1):34–39.
19. Hida T, Tamiya M, Nishio M, et al. Phase I study of intravenous ASA404 (vadimezan) administered in combination with paclitaxel and carboplatin in Japanese patients with non-small cell lung cancer. *Cancer Sci*. 2011;102(4):845–851.
20. McKeage MJ, Reck M, Jameson MB, et al. Phase II study of ASA404 (vadimezan, 5,6-dimethylxanthenone-4-acetic acid/DMXAA) 1800 mg/m(2) combined with carboplatin and paclitaxel in previously untreated advanced non-small cell lung cancer. *Lung Cancer*. 2009;65(2):192–197.
21. Prantner D, Perkins DJ, Lai W, et al. 5,6-Dimethylxanthenone-4-acetic acid (DMXAA) activates stimulator of interferon gene (STING)-dependent innate immune pathways and is regulated by mitochondrial membrane potential. *J Biol Chem*. 2012;287(47):39776–39788.
22. Conlon J, Burdette DL, Sharma S, et al. Mouse, but not human STING, binds and signals in response to the vascular disrupting agent 5,6-dimethylxanthenone-4-acetic acid. *J Immunol*. 2013;190(10):5216–5225.
23. Gao P, Zillinger T, Wang W, et al. Binding-pocket and lid-region substitutions render human STING sensitive to the species-specific drug DMXAA. *Cell Rep*. 2014;8(6):1668–1676.
24. Diaz-Moralli S, Tarrado-Castellarnau M, Miranda A, Cascante M. Targeting cell cycle regulation in cancer therapy. *Pharmacol Ther*. 2013;138(2):255–271.
25. Ong SE, Mann M. Stable isotope labeling by amino acids in cell culture for quantitative proteomics. *Methods Mol Biol*. 2007;359:37–52.
26. Mann M. Functional and quantitative proteomics using SILAC. *Nat Rev Mol Cell Biol*. 2006;7(12):952–958.
27. Ong SE. The expanding field of SILAC. *Anal Bioanal Chem*. 2012;404(4):967–976.
28. Ong SE, Mann M. A practical recipe for stable isotope labeling by amino acids in cell culture (SILAC). *Nat Protoc*. 2006;1(6):2650–2660.
29. Farazi TA, Hoell JI, Morozov P, Tuschl T. MicroRNAs in human cancer. *Adv Exp Med Biol*. 2013;774:1–20.
30. Mariño G, Niso-Santano M, Baehrecke EH, Kroemer G. Self-consumption: the interplay of autophagy and apoptosis. *Nat Rev Mol Cell Biol*. 2014;15(2):81–94.
31. Shanware NP, Bray K, Abraham RT. The PI3K, metabolic, and autophagy networks: interactive partners in cellular health and disease. *Annu Rev Pharmacol Toxicol*. 2013;53:89–106.
32. Morgensztern D, McLeod HL. PI3K/Akt/mTOR pathway as a target for cancer therapy. *Anticancer Drugs*. 2005;16(8):797–803.
33. Wu WK, Coffelt SB, Cho CH. The autophagic paradox in cancer therapy. *Oncogene*. 2012;31(8):939–953.
34. Ferreira CG, Epping M, Kruyt FA, Giaccone G. Apoptosis: target of cancer therapy. *Clin Cancer Res*. 2002;8(7):2024–2034.
35. Fulda S, Galluzzi L, Kroemer G. Targeting mitochondria for cancer therapy. *Nat Rev Drug Discov*. 2010;9(6):447–464.
36. Heavey S, O'Byrne KJ, Gately K. Strategies for co-targeting the PI3K/Akt/mTOR pathway in NSCLC. *Cancer Treat Rev*. 2014;40(3):445–456.
37. Ellis L, Shah P, Hammers H, et al. Vascular disruption in combination with mTOR inhibition in renal cell carcinoma. *Mol Cancer Ther*. 2012;11(2):383–392.
38. Brauer R, Wang LC, Woon ST, et al. Labeling of oxidizable proteins with a photoactivatable analog of the antitumor agent DMXAA: evidence for redox signaling in its mode of action. *Neoplasia*. 2010;12(9):755–765.
39. Keum YS, Choi BY. Molecular and chemical regulation of the Keap1-Nrf2 signaling pathway. *Molecules*. 2014;19(7):10074–10089.
40. Ma Q. Role of Nrf2 in oxidative stress and toxicity. *Annu Rev Pharmacol Toxicol*. 2013;53:401–426.
41. Taylor RC, Cullen SP, Martin SJ. Apoptosis: controlled demolition at the cellular level. *Nat Rev Mol Cell Biol*. 2008;9(3):231–241.
42. Estaquier J, Vallette F, Vayssiere JL, Mignotte B. The mitochondrial pathways of apoptosis. *Adv Exp Med Biol*. 2012;942:157–183.
43. Kang R, Zeh HJ, Lotze MT, Tang D. The Beclin 1 network regulates autophagy and apoptosis. *Cell Death Differ*. 2011;18(4):571–580.
44. Maiuri MC, Criollo A, Kroemer G. Crosstalk between apoptosis and autophagy within the Beclin 1 interactome. *EMBO J*. 2010;29(3):515–516.
45. Kabeya Y, Mizushima N, Ueno T, et al. LC3, a mammalian homologue of yeast Apg8p, is localized in autophagosome membranes after processing. *EMBO J*. 2000;19(21):5720–5728.
46. Downey CM, Aghaei M, Schwendener RA, Jirik FR. DMXAA causes tumor site-specific vascular disruption in murine non-small cell lung cancer, and like the endogenous non-canonical cyclic dinucleotide STING agonist, 2′3′-cGAMP, induces M2 macrophage repolarization. *PLoS One*. 2014;9(6):e99988.
47. Zhang SH, Zhang Y, Shen J, et al. Tumor vascular disrupting agent 5,6-dimethylxanthenone-4-acetic acid inhibits platelet activation and thrombosis via inhibition of thromboxane A_2 signaling and phosphodiesterase. *J Thromb Haemost*. 2013;11(10):1855–1866.
48. Kim S, Peshkin L, Mitchison TJ. Vascular disrupting agent drug classes differ in effects on the cytoskeleton. *PLoS One*. 2012;7(7):e40177.
49. Shirey KA, Nhu QM, Yim KC, et al. The anti-tumor agent, 5,6-dimethylxanthenone-4-acetic acid (DMXAA), induces IFN-β-mediated antiviral activity in vitro and in vivo. *J Leukoc Biol*. 2011;89(3):351–357.
50. Woon ST, Hung SS, Wu DC, et al. NF-κB-independent induction of endothelial cell apoptosis by the vascular disrupting agent DMXAA. *Anticancer Res*. 2007;27(1A):327–334.

51. Siemann DW, Chaplin DJ, Horsman MR. Vascular-targeting therapies for treatment of malignant disease. *Cancer*. 2004;100(12):2491–2499.
52. Dolai S, Xu Q, Liu F, Molloy MP. Quantitative chemical proteomics in small-scale culture of phorbol ester stimulated basal breast cancer cells. *Proteomics*. 2011;11(13):2683–2692.
53. Geiger T, Cox J, Ostasiewicz P, Wisniewski JR, Mann M. Super-SILAC mix for quantitative proteomics of human tumor tissue. *Nat Methods*. 2010; 7(5):383–385.
54. Everley PA, Krijgsveld J, Zetter BR, Gygi SP. Quantitative cancer proteomics: stable isotope labeling with amino acids in cell culture (SILAC) as a tool for prostate cancer research. *Mol Cell Proteomics*. 2004;3(7): 729–735.
55. Doherty MK, Hammond DE, Clague MJ, Gaskell SJ, Beynon RJ. Turnover of the human proteome: determination of protein intracellular stability by dynamic SILAC. *J Proteome Res*. 2009;8(1): 104–112.
56. Hammond DE, Hyde R, Kratchmarova I, Beynon RJ, Blagoev B, Clague MJ. Quantitative analysis of HGF and EGF-dependent phosphotyrosine signaling networks. *J Proteome Res*. 2010;9(5):2734–2742.
57. Duan X, Kelsen SG, Clarkson AB Jr, Ji R, Merali S. SILAC analysis of oxidative stress-mediated proteins in human pneumocytes: new role for treacle. *Proteomics*. 2010;10(11):2165–2174.
58. Coombs KM, Berard A, Xu W, et al. Quantitative proteomic analyses of influenza virus-infected cultured human lung cells. *J Virol*. 2010;84(20):10888–10906.
59. Munday DC, Hiscox JA, Barr JN. Quantitative proteomic analysis of A549 cells infected with human respiratory syncytial virus subgroup B using SILAC coupled to LC-MS/MS. *Proteomics*. 2010; 10(23):4320–4334.
60. Foster MW, Thompson JW, Forrester MT, et al. Proteomic analysis of the NOS2 interactome in human airway epithelial cells. *Nitric Oxide*. 2013;34:37–46.
61. Wu Q, Xu W, Cao L, et al. SAHA treatment reveals the link between histone lysine acetylation and proteome in nonsmall cell lung cancer A549 cells. *J Proteome Res*. 2013;12(9):4064–4073.
62. Chiu HC, Hannemann H, Heesom KJ, Matthews DA, Davidson AD. High-throughput quantitative proteomic analysis of dengue virus type 2 infected A549 cells. *PLoS One*. 2014;9(3):e93305.
63. Gray TA, Alsamman K, Murray E, Sims AH, Hupp TR. Engineering a synthetic cell panel to identify signalling components reprogrammed by the cell growth regulator anterior gradient-2. *Mol Biosyst*. 2014; 10(6):1409–1425.
64. Bunz F, Dutriaux A, Lengauer C, et al. Requirement for p53 and p21 to sustain G_2 arrest after DNA damage. *Science*. 1998;282(5393): 1497–1501.
65. Hunter T. Protein kinases and phosphatases: the yin and yang of protein phosphorylation and signaling. *Cell*. 1995;80(2):225–236.
66. Boehning D, Patterson RL, Sedaghat L, Glebova NO, Kurosaki T, Snyder SH. Cytochrome c binds to inositol (1,4,5) trisphosphate receptors, amplifying calcium-dependent apoptosis. *Nat Cell Biol*. 2003; 5(12):1051–1061.
67. Yang J, Liu X, Bhalla K, et al. Prevention of apoptosis by Bcl-2: release of cytochrome c from mitochondria blocked. *Science*. 1997;275(5303): 1129–1132.
68. Jeffers JR, Parganas E, Lee Y, et al. Puma is an essential mediator of p53-dependent and -independent apoptotic pathways. *Cancer Cell*. 2003;4(4):321–328.
69. Fesik SW, Shi Y. Structural biology. Controlling the caspases. *Science*. 2001;294(5546):1477–1478.
70. Klionsky DJ, Emr SD. Autophagy as a regulated pathway of cellular degradation. *Science*. 2000;290(5497):1717–1721.
71. Chen Y, Yu L. Autophagic lysosome reformation. *Exp Cell Res*. 2013;319(2):142–146.
72. Denton D, Nicolson S, Kumar S. Cell death by autophagy: facts and apparent artefacts. *Cell Death Differ*. 2012;19(1):87–95.
73. Suzuki T, Motohashi H, Yamamoto M. Toward clinical application of the Keap1-Nrf2 pathway. *Trends Pharmacol Sci*. 2013;34(6):340–346.
74. Kensler TW, Wakabayashi N, Biswal S. Cell survival responses to environmental stresses via the Keap1-Nrf2-ARE pathway. *Annu Rev Pharmacol Toxicol*. 2007;47:89–116.